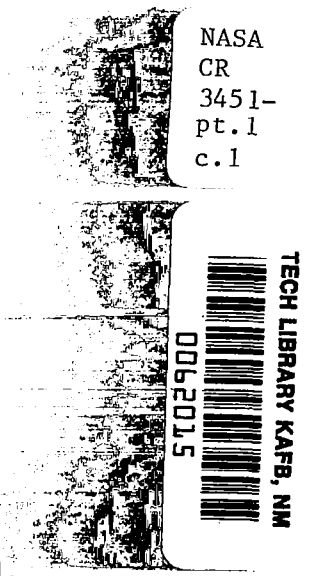

NASA Contractor Report 3451

Terminal Area Automatic Navigation, Guidance, and Control Research Using the Microwave Landing System (MLS)

Part 1 - Automatic Rollout, Turnoff, and Taxi

Samuel Pines

CONTRACT NAS1-15116
AUGUST 1981

NASA

NASA Contractor Report 3451

Terminal Area Automatic Navigation, Guidance, and Control Research Using the Microwave Landing System (MLS)

Part 1 - Automatic Rollout, Turnoff, and Taxi

Samuel Pines
Analytical Mechanics Associates, Inc.
Hampton, Virginia

Prepared for
Langley Research Center
under Contract NAS1-15116

National Aeronautics
and Space Administration

**Scientific and Technical
Information Branch**

1981

TABLE OF CONTENTS

LIST OF FIGURES

LIST OF FIGURES (Concluded)

LIST OF TABLES

SUMMARY

This report contains the results of a study developed for the Langley TCV B-737 program to apply existing navigation aids plus magnetic leader cable signals and develop braking and reverse thrust guidance laws to provide for rapid automated rollout, turnoff, and taxi to reduce runway occupation time for a wide variety of landing conditions for conventional commercial-type aircraft.

The study concludes that it is possible and feasible to execute rollout and turnoffs on conventional runways in under 25 seconds with an integrated automated landing deceleration system for a large variety of aircraft and runway landing conditions.

Closed loop guidance laws for braking and reverse thrust are derived for rollout, turnoff, and taxi, as functions of the landing speed, the desired taxi speed and the distance to go. Brake limitations for wet runway conditions and reverse thrust limitations are taken into account to provide decision rules to avoid tire skid and to choose an alternate turnoff point, farther down the runway, to accommodate extreme landing conditions.

The ground rules underlying the guidance policy are:

1) To exit the rollout runway in under 25 seconds, if possible;
2) The guidance shall be closed loop, using the brakes as a modulating feed back device in coordination with reverse thrust to achieve the desired deceleration;
3) To avoid using brake pressures that induce the skid;
4) To decelerate mainly with reverse thrust using modulated braking for fine control and using nominal braking only when the maximum specified reverse thrust cannot decelerate the aircraft to the specified exit speed.

This study was carried out for the TCV B737 aircraft and may be readily adapted to most conventional commercial aircraft.

INTRODUCTION

In order to reduce runway occupation time in rollout and turnoff it is desired to generate an automated uniform braking and reverse thrust guidance policy that will accommodate a large range of landing speeds, landing weights and runway conditions. To take full advantage of the aircraft capability in reverse thrust and braking it is necessary to base such a guidance policy on a fairly accurate model of the dynamic action of these control forces.

No serious difficulty is encountered in generating a deceleration policy for dry, or even damp, runways in rollout and turnoff given the availability of brakes and reverse thrust (Ref. 1). However, for flooded runway conditions, hydroplaning in the ground speed range above 100 knots will negate the use of brakes. Moreover, the effective side force tire coefficient is rendered ineffective on flooded runways above 80 knots.

While it is possible to generate different guidance laws for dry and wet runways, it is preferable to devise a uniform policy, if at all possible. Such a policy is derived herein.

Due to the stringent demands on time and space it is necessary to employ navigation aids such as MLS, buried magnetic leader cables, aircraft sensors and modern digital computer techniques to ensure safe and stable execution of the rollout, turnoff, and taxi commands.

The detail description of the aircraft landing dynamics and navigation system (INS, MLS and the buried magnetic leader cable and aircraft sensors) is contained in Refs. 2 and 3, and is not repeated in this report.

The report contains the derivation of the guidance laws and the results of the simulation for a variety of aircraft and runway landing conditions.

I. AIRCRAFT DECELERATION MODEL FOR BRAKING AND REVERSE THRUST

For the purposes of modeling the deceleration of an aircraft in rollout, prior to turnoff, it is sufficiently accurate to treat the aircraft as a point mass in a single degree of freedom acting under the effects of drag, reverse thrust and braking.

Let x be the position of the aircraft along the single degree-of-freedom coordinate, $\dot{x}$ its velocity and $\ddot{x}$, the acceleration. Then, we have for the deceleration of the point mass

$$\ddot{x} = -\frac{1}{2m}\rho s C_D \dot{x}^2 - \mu_R g - \mu_B H(\dot{x}_B) g + \frac{k}{m} \tag{1}$$

where

μ_R	is the rolling friction coefficient
μ_B	is the tire braking friction coefficient
$H(\dot{x}_B)$	is the heaviside operator initiated at the instant of braking command
$\dot{x}_B$	is the velocity at which braking is first permitted
k	is the thrust
m	is the aircraft point mass
g	is the gravitational constant
s	is the effective aircraft wing area
ρ	is the mean air mass density
C_D	is the drag coefficient in the landing configuration

To integrate Eq. (1) we require the time history of the thrust, $k(t)$, and the velocity $\dot{x}(t)$.

In the case of the thrust, we model the thrust system as a first order servo with a response time, τ . Given a desired reverse thrust command, k_D , we have

$$\frac{k}{m} = \frac{1}{m}\left(k_D + (k_o - k_D)\, e^{-t/\tau}\right) \tag{2}$$

where

k_o is the thrust at the time of the reverse thrust command.

To integrate the drag term, we make use of the concept of averaging. The average squared velocity may be estimated from the assumption of a constant deceleration

$$\frac{\int_o^t \dot{x}^2\, dt}{\int_o^t dt} \simeq \frac{\int_{\dot{x}(o)}^{\dot{x}(t)} \dot{x}^2\, d\dot{x}}{\int_{\dot{x}(o)}^{\dot{x}(t)} d\dot{x}} \tag{3}$$

Thus we have

$$\int_o^t \dot{x}^2\, dt = \frac{\dot{x}^3(t) - \dot{x}^3(o)}{3\left(\dot{x}(t) - \dot{x}(o)\right)}\, t = \frac{t}{3}\left(\dot{x}^2(t) + \dot{x}(t)\,\dot{x}(o) + \dot{x}^2(o)\right) \tag{4}$$

Employing Eq's. (2) and (4) we have for the integration of Eq. (1)

$$\dot{x} - \dot{x}_o = \left\{ \begin{array}{l} -\frac{\rho\, s C_D}{6m}\left(\dot{x}^2 + \dot{x}\,\dot{x}_o + \dot{x}_o^2\right) t - \mu_R\, g\, t \\ -\mu_B\, g\, H(\dot{x}_B)\,(t - t_B) \\ +\frac{1}{m}\left((k_o - k_D)\,\tau\,(1 - e^{-t/\tau}) + k_D\, t\right) \end{array} \right\} \tag{5}$$

where t_B is the time of brake initiation.

II. REVERSE THRUST AND BRAKING GUIDANCE FOR ROLLOUT AND TURNOFF

Since the reverse thrust has a relatively long response time, it can not be used as a real time closed loop control variable. The brakes, however, do possess good response characteristics. The philosophy used in generating a closed loop deceleration guidance law is to set the reverse thrust command at an average open loop deceleration level, well within its deceleration capability, and to utilize the brakes in a closed loop mode to realize a combined average constant desired deceleration.

For this purpose, Eq. (5) may be used to solve for the desired reverse thrust, k_D, that must be called for in order to reach the desired turn speed, $\dot{x}_T$, at the same time the aircraft reaches a desired position, x_D. For this purpose, we assume that only the rolling friction is acting and that $\mu_B = 0$. To estimate the deceleration time, t, we use the assumption of constant deceleration, for which t is given by

$$t = \frac{2\left[x_D - x_o - D_B - (t_s V_G/1.25)\right]}{\dot{x}_T + \dot{x}_o} \tag{6}$$

where D_B is a specified distance prior to turnoff when braking and reverse thrust are not desired (in effect a safety margin) and t_s is a time over when the brake pressure is increased to its nominal value.

Finally, since $t >> \tau$, we have

$$1 - e^{-t/\tau} \simeq 1 \tag{7}$$

The desired reverse thrust, k_D, is given by

$$k_D = \frac{1}{1 - \tau/t} \left\{ \begin{array}{l} \dfrac{m(\dot{x}_T - \dot{x}_o) - \tau k_o}{t} \\ + \dfrac{\rho s C_D}{6} (\dot{x}_T^2 + \dot{x}_o^2 + \dot{x}_o \dot{x}_T) + \mu_R W \end{array} \right\} \tag{8}$$

where $\dot{x}_T$ is the desired turn speed

$x_D - x_o$ is the distance to go to the turnoff point

W is the aircraft weight

In the event that the called for reverse thrust exceeds the maximum reverse thrust, an estimate is made to see if the excess desired acceleration can be approximately achieved with additional braking. If it can, we set the command reverse thrust to K_{MAX} and proceed.

The computation for the possible brake deceleration addition is given below:

$$K_\Delta = K_D + |K_{MAX}| \tag{9}$$

The possible brake friction coefficient is acceptable if:

For dry and damp runways

$$\mu_p = \frac{|K_\Delta|}{W} + .02 \leq .4 \tag{10a}$$

where .02 is an arbitrary brake coefficient safety factor.

For wet and icy runways

$$\mu_p = \frac{|K_\Delta|}{W} \leq .025 \frac{\dot{x}_T + \dot{x}_H}{\dot{x}_T + \dot{x}} \tag{10b}$$

Where we have that the hydroplane speed is given by

$$\dot{x}_H \text{ (KNOTS)} = 9\sqrt{\text{tire pressure}} \qquad \text{(Ref. 1)} \tag{11}$$

In the event the test fails, we call for the next turnoff runway down the runway, and recompute the reverse thrust command utilizing the extended distance to go, $x_{D2} - x_o$.

When the turning speed has been achieved, the thrust command is set to ensure a set taxi speed, $\dot{x}_{TX}$, opposing the deceleration forces of drag and rolling friction. Thus, we have for the taxi phase, the desired thrust for taxi, k_T, is given by

$$k_T = \frac{1}{2} \rho s C_D \dot{x}_{TX}^2 + \mu_R W \tag{12}$$

where the nominal value of $\mu_R = .015$.

The braking law is designed to achieve and maintain a uniform average acceleration to reach the desired $\dot{x}_T$, at the desired position, x_D, given the present acceleration velocity and position. The block diagram of the braking law is shown in Figure 1.

We have for the average desired acceleration

$$\ddot{x}_D = \frac{\dot{x}_T^2 - \dot{x}^2}{2 \text{ (DIST)}} \tag{13}$$

where DIST is defined as

$$\text{DIST} = \begin{cases} \text{Distance to turnoff point} - D_B \\ \\ \text{7 meter (50) if DIST} \leq \text{7 meters} \end{cases} \tag{13a}$$

The braking feed back law is designed to maintain the constant desired deceleration. Let the error in the braking coefficient , μ_e , be given by

$$0 < \mu_e = \frac{\ddot{x} - \ddot{x}_D}{g} \tag{13b}$$

The commanded braking coefficient , μ_c , is obtained from the solution of the differential equation

$$\frac{d}{dt}\ \mu_c = K\ \mu_e\ ,\quad K = 2 \tag{14}$$

The commanded brake coefficient is limited to prevent excessive braking under dry conditions and to prevent skidding under wet conditions as follows:

For dry runways

$$0 \leq \mu_c \leq \mu_L = .4 \tag{14a}$$

For wet runways

$$\mu_c = \left\{ \begin{array}{l} 0 \text{ for } \dot{x} > \dot{x}_H \\ \\ \dfrac{.014\,\dot{x} + 1.}{.14\,\dot{x} + 2.} \leq .4 \text{ for } \dot{x} \leq \dot{x}_H \end{array} \right\} \tag{14b}$$

where $\dot{x}_H$ is the hydroplaning speed.

The brake command is ramped to its nominal value during the first t_s seconds of brake initiation where t_s is a specified parameter (t_s = 1 second). At t_s seconds after brake initiation, the control law is switched into the control loop and the rate command integrator is initialized to the nominal brake coefficient, μ_{nom} computed either in equation (10a) or (10b).

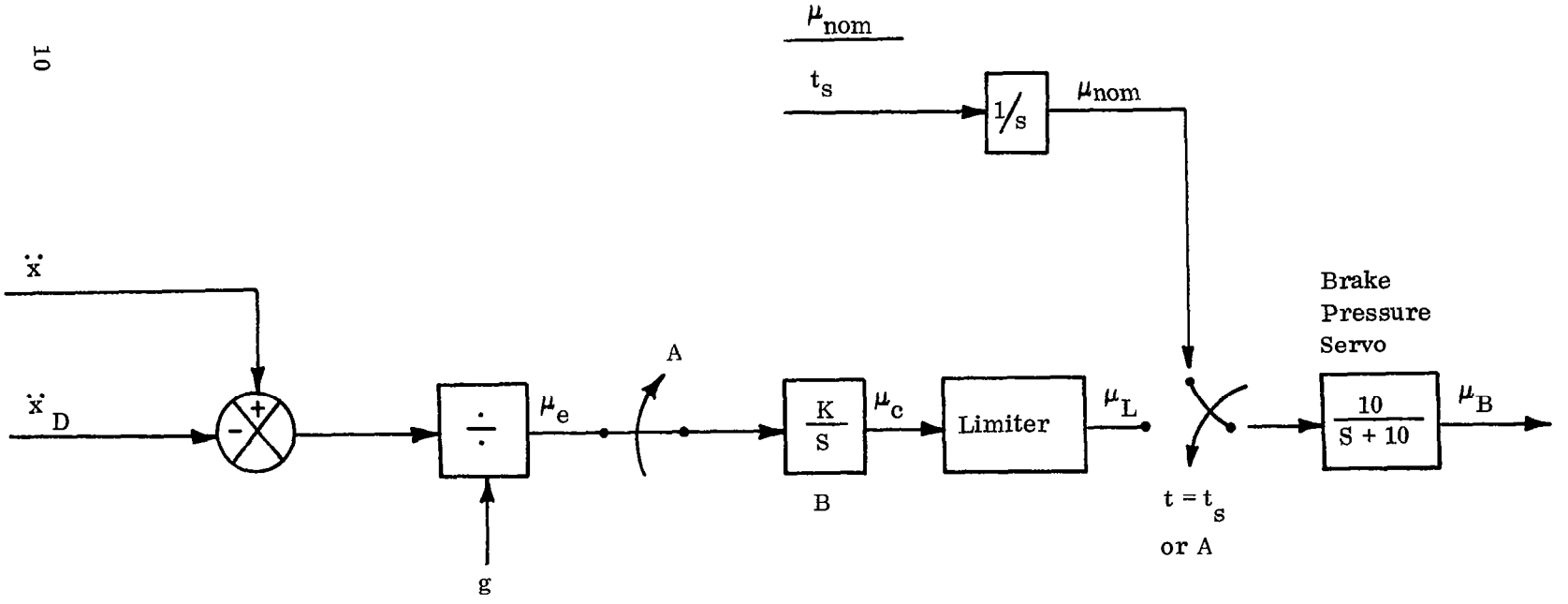

μ_{nom} - computed nominal braking coefficient

t_s - time to apply nominal brake pressure

μ_L - limited brake pressure; for dry runway set equal to .4

for wet runway set equal to $\frac{.014\,\dot{x} + 1}{.14\,\dot{x} + 2}$

A - if wet runway and ground speed greater than hydroplane speed

B - initialize integrator at t_s to μ_{nom}

Figure 1. Closed Loop Braking Law

III. STEERING GUIDANCE FOR ROLLOUT TURNOFF AND TAXI

The object of the steering guidance logic is to direct the aircraft to follow a given sequence of straight lines and curves from touchdown to turn-off to taxi in a short time span so as to safely reduce runway occupancy. In a manner completely equivalent to the in flight way point RNAV equations, we fix a set of runway coordinate points consisting of the beginning and end of each segment. See Figures 2a and 2b.

The guidance parameters to be determined on each segment consist of the following:

1) Cross track error (CTE)
2) Cross track rate error (CTRE)
3) Track angle error (TAE)
4) Yaw rate error (YRE)
5) Distance to go to the next way point (DTGO)
6) Time to go to the next segment (TTGO)

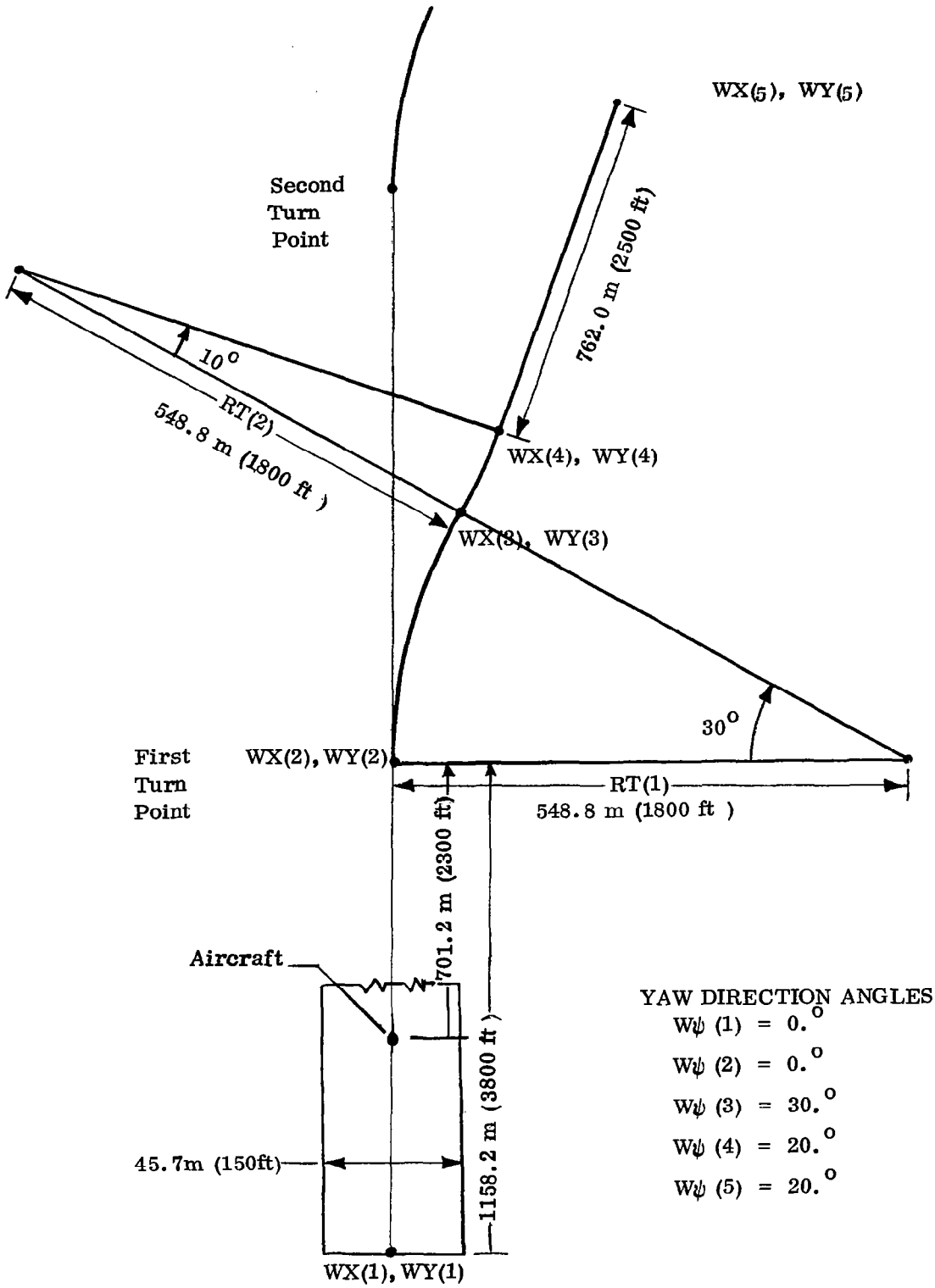

Figure 2(a). Rollout and Turnoff Geometry

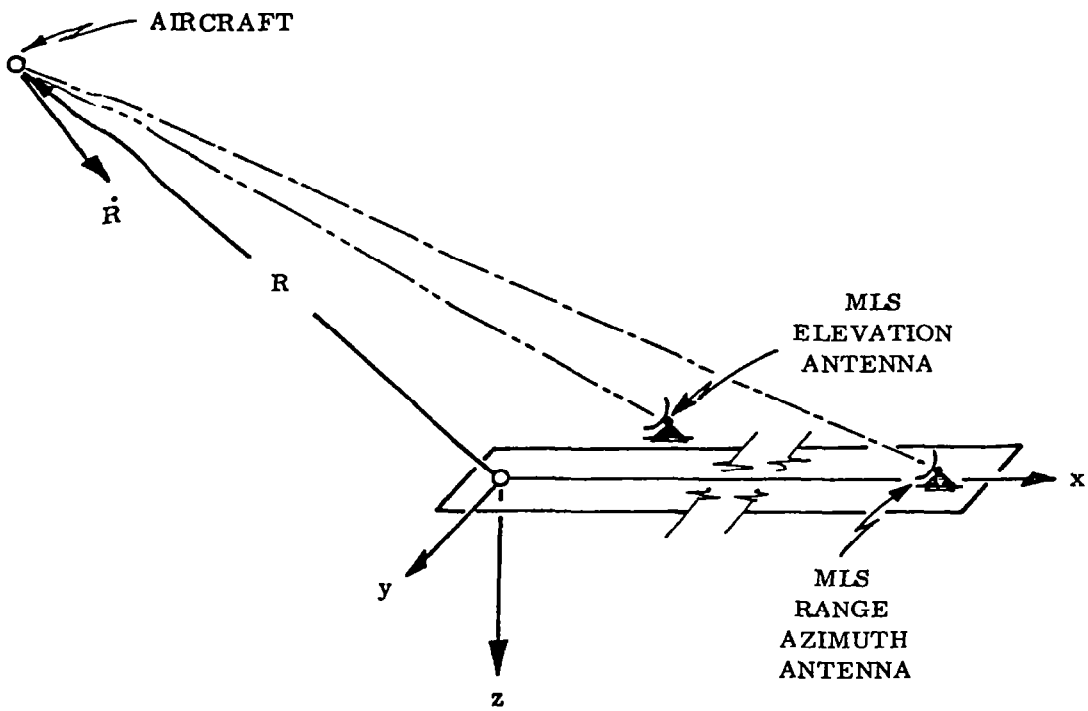

Figure 2 (b). Runway (Inertial) Coordinates and Aircraft Position, Velocity Vectors ($R, \dot{R}$)

From the navigation system we may obtain the best estimate of aircraft position, velocity and acceleration in runway coordinates ($\hat{x}$, $\hat{y}$, $\hat{\dot{x}}$, $\hat{\dot{y}}$, $\hat{\ddot{x}}$, $\hat{\ddot{y}}$) as well as the aircraft yaw and yaw rate ($\hat{\psi}$, $\hat{r}$). The on board computer contains the coordinates of the way points (WX(I), WY(I)) , the yaw heading angle ($W\psi(I)$) at the ith segment, and the length of each segment, LSG(I).

The guidance parameters are detailed below, (1) for straight line segments, (2) for circular segments and finally (3) for centered parabolic segments. (See Appendix A).

The aircraft deviations from the desired location on runway track (TX , TY) is not necessarily computed with respect to the cg of the aircraft, but rather with respect to a sensor on the aircraft center line, (AXP , AZP), whose location is chosen to be in a logical belly location of the aircraft. (See Figure 3).

The coordinates of the aircraft sensor in runway coordinates is given by

$$\begin{aligned} XRP &= \hat{x} + \cos(\hat{\psi})\, AXP \\ YRP &= \hat{y} + \sin(\hat{\psi})\, AXP \end{aligned} \tag{15}$$

The coordinates of sensor velocity in runway coordinates is given by

$$\begin{aligned} \dot{XRP} &= \hat{\dot{x}} - \sin(\hat{\psi})\, AXP\ \hat{r} \\ \dot{YRP} &= \hat{\dot{y}} + \cos(\hat{\psi})\, AXP\ \hat{r} \end{aligned} \tag{16}$$

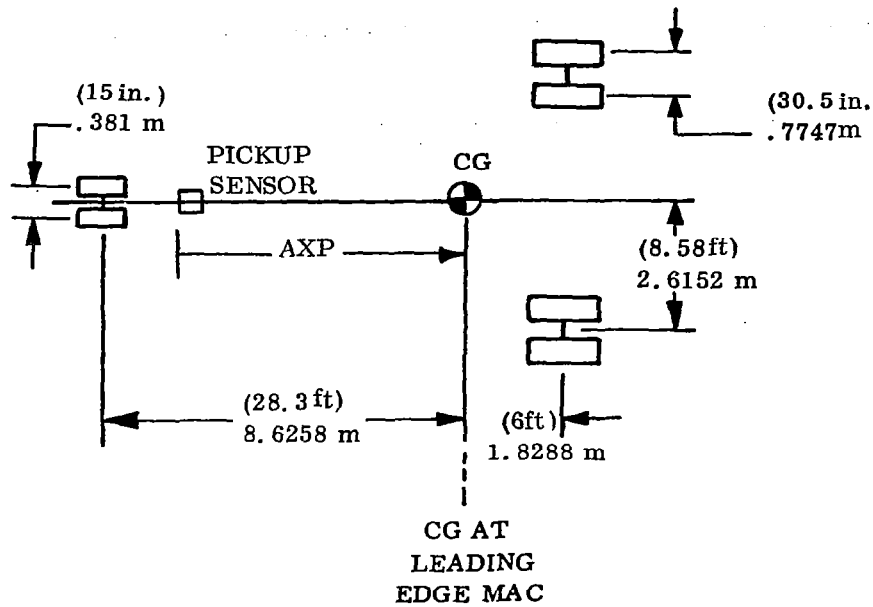

LANDING GEAR LOCATION

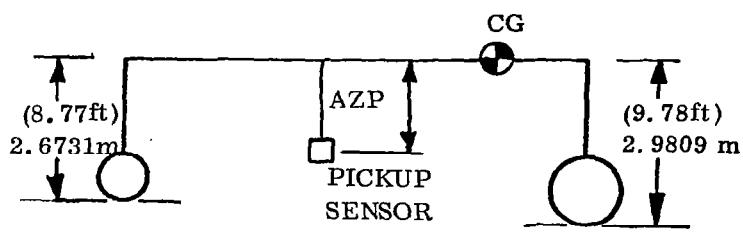

EXTENDED GEAR HEIGHTS

Figure 3. Landing Gear Geometry

(1) Straight Line Segments

$$CTE = \left(YRP - WY(I)\right)\cos\left(W\psi(I)\right) - \left(XRP - WX(I)\right)\sin\left(W\psi(I)\right) \tag{17a}$$

$$CTRE = \dot{YRP}\cos\left(W\psi(I)\right) - \dot{XRP}\sin\left(W\psi(I)\right) \tag{17b}$$

$$TAE = \left(\psi - W\psi(I)\right)\frac{180}{\pi} \tag{17c}$$

$$YRE = \hat{r}\,\frac{180}{\pi} \tag{17d}$$

$$DTGO = LSG(I) - \left(YRP - WY(I)\right)\sin\left(W\psi(I)\right) - \left(XRP - WX(I)\right)\cos\left(W\psi(I)\right) \tag{17e}$$

$$TGO = DTGO \Big/ \left(\hat{\dot{x}}^2 + \hat{\dot{y}}^2\right)^{1/2} \tag{17f}$$

where

LSG(I) = length of the Ith straight segment

RAD = $180./\pi$

WX(I) , WY(I) , $W\psi(I)$ are defined at start of each segment.

The time to go equation is common to all segment types.

A test is made to switch to the guidance parameter logic for the next segment whenever

$$TGO \leq .05 \text{ second} \tag{18}$$

(2) Circular Segments

The desired runway track coordinates for the circular turn are computed from the intersection of the circular track and the radial vector from the center of the turn circle through the best estimate of the aircraft position.

The coordinates of turn circle center are given by

$$\begin{aligned} CTX(I) &= WX(I) - SGN(I)\ RT(I)\ \sin\left(W\psi(I)\right) \\ CTY(I) &= WY(I) + SGN(I)\ RT(I)\ \cos\left(W\psi(I)\right) \end{aligned} \tag{19}$$

when $SGN(I) = +1.$ for a right hand turn

$= -1.$ for a left hand turn

and $RT(I)$ = radius of the turn

The coordinates of the radius vector from the turn center to the aircraft sensor are given by

$$\left.\begin{aligned} XS &= XRP - CTX(I) \\ YS &= YRP - CTY(I) \end{aligned}\right\} \tag{20}$$

$$CTE = SGN(I)\left[RT(I) - (XS^2 + YS^2)^{\frac{1}{2}}\right] \tag{21a}$$

$$CTRE = -SGN(I)\ (XS\ \dot{X}RP + YS\ \dot{Y}RP) \Big/ (XS^2 + YS^2)^{\frac{1}{2}} \tag{21b}$$

$$TAE = TAN^{-1}\left\{\frac{XS\cos(\hat{\psi}) + YS\sin(\hat{\psi})}{YS\cos(\hat{\psi}) - XS\sin(\hat{\psi})}\right\}\frac{180}{\pi} \tag{21c}$$

$$YRE = \left[\hat{r} - (\hat{\dot{x}}^2 + \hat{\dot{y}}^2)^{\frac{1}{2}}\ SGN(I)/RT(I)\right]\frac{180}{\pi} \tag{21d}$$

$$DTGO = RT(I)\left|\psi_{DS} - W\psi(I+1)\right| \tag{21e}$$

where

$$\psi_{DS} - W\psi(I+1) = \tan^{-1}\left\{\frac{-\sin(W\psi(I+1)\ YS - \cos(W\psi(I+1)\ XS}{-\cos(W\psi(I+1)\ YS + \sin(W\psi(I+1)\ XS}\right\} \tag{21f}$$

The concept of a parabolic turn segment is introduced in order to attempt to reduce the severity of the initiation of the yaw rate onset during a fast turnoff. It represents an "easy on" and "easy off" for a turn and reserves the maximum turn rate for the center of the turn. The theory and derivation is contained in Appendix A. The guidance parameter equations are detailed below.

(3) Centered Parabolic Segments

The desired position on the parabolic track is most conveniently described in a Cartesian coordinate system whose origin is at the middle of the parabolic turn as described and illustrated in Appendix A. The desired position on the parabola requires the solution of a cubic polynomial. The equations must be solved in real time and are outlined below:

The vector from the start of the parabola to the aircraft sensor in runway coordinates is given by

$$\left.\begin{aligned} XS &= XRP - WX(I) \\ YS &= YRP - WY(I) \end{aligned}\right\} \qquad (22)$$

Let

$$\alpha = \frac{W\psi(I) + W\psi(I+1)}{2}$$

$$\beta = \frac{W\psi(I+1) - W\psi(I)}{2}$$

$$RP(I) = \left| \frac{\cos\alpha\,(WX(I+1) - WX(I)) + \sin\,(WY(I+1) - WY(I))}{2\tan\beta} \right| \qquad (23)$$

$$XPAI = -SGN(I)\, RP(I) \tan\beta$$

$$YPAI = 1/2\, XPAI \tan\beta$$

The coordinates of the aircraft sensor in the centered parabolic system are

$$XPA = XPAI + XS \cos \alpha + YS \sin \alpha$$

$$YPA = YPAI - XS \sin \alpha + YS \cos \alpha$$

The desired position on the parabolic track in centered coordinates is given by

$$XD = \frac{AQ}{|AQ|^{2/3}} + \frac{BQ}{|BQ|^{2/3}}$$

$$YD = 1/2 \frac{(XD)^2}{RP(I)} SGN(I)$$

where:

$$AQ = -HQ + SQ$$

$$BQ = -HQ - SQ$$

$$SQ = \left(\frac{DISC}{108.}\right)^{1/2}$$

$$HQ = 1/2\ XAQ$$

$$DISC = 4\ XAP^3 + 27\ XAQ^2$$

$$XAQ = -2\ RP^2(I)\ XPA$$

$$XAP = 2\ RP(I)\left(RP(I) - YPA\ SGN(I)\right)$$

The desired yaw heading at the desired track position in the parabolic system is given by

$$\sin \psi_{DP} = SGN(I) \frac{XD}{(XD^2 + RP^2)^{1/2}}$$

$$\cos \psi_{DP} = \frac{RP}{(XD^2 + RP^2)^{1/2}}$$

The desired heading in the runway system is given by

$$\psi_D = \psi_{DP} + \alpha \tag{27}$$

The desired yaw rate on the track is given by

$$r_D = \frac{(\hat{\dot{x}}^2 + \hat{\dot{y}}^2)^{\frac{1}{2}} \, SGN(I)}{(XD^2 + RP^2)^{\frac{1}{2}}} \tag{28}$$

In terms of the above we may now compute the required guidance parameters

$$CTE = (YPA - YD) \cos(\psi_{DP}) - (XPA - XD \sin(\psi_{DP}) \tag{29a}$$

$$CTRE = \dot{Y}RP \cos\psi_D - \dot{X}RP \sin\psi_D$$

$$-r_D\left(YPA \sin\psi_{DP} + XPA \cos\psi_{DP}\right)$$

$$-r_D\left(-1/2 \, SGN(I) \, RP(I) \sin\psi_{DP} \left(1 + \frac{1}{\cos^2\psi_{DP}}\right)\right) \tag{29b}$$

$$TAE = \tan^{-1}\left[\frac{(\sin\hat{\psi}\cos\psi_D - \cos\hat{\psi}\sin\psi_D)}{(\cos\hat{\psi}\cos\psi_D + \sin\hat{\psi}\sin\psi_D)}\right]\frac{180}{\pi} \tag{29c}$$

$$YRE = \hat{r} - r_D \tag{29d}$$

$$DTGO = 1/2\left(LGS(I) - SGN(I) \, RP(I)\left(\frac{\sin\psi_{DP}}{\cos^2\psi_{DP}} + \ln\frac{1+\sin\psi_{DP}}{\cos\psi_{DP}}\right)\right) \tag{29e}$$

With the buried magnetic leader cable in operation the cross track error and the track angle error may be taken directly from the voltage output of the three magnetic coils situated at sensor locations. The details of theory of the magnetic cable and sensor are described in Refs. (2) and (3).

Let the voltages from the output of the three coils be v_x, v_y, and v_z, then we may obtain directly

$$CTE = (ZP - Z_{WIRE}) \frac{v_z}{v_y} \tag{30}$$

$$TAE = \frac{v_x}{v_y} \tag{31}$$

when $ZP - Z_{WIRE}$ is a known height of the pickup above the buried cable.

The steering law is a slight modification of the Boeing B737 rollout equation which uses a nose wheel command geared to the rudder signal by the ratio of

$$\delta_{NW_{COM}} = -7/26 \; \delta_{RUD_{COM}} \tag{32}$$

The block diagram for the steering law is given in Fig. 4.

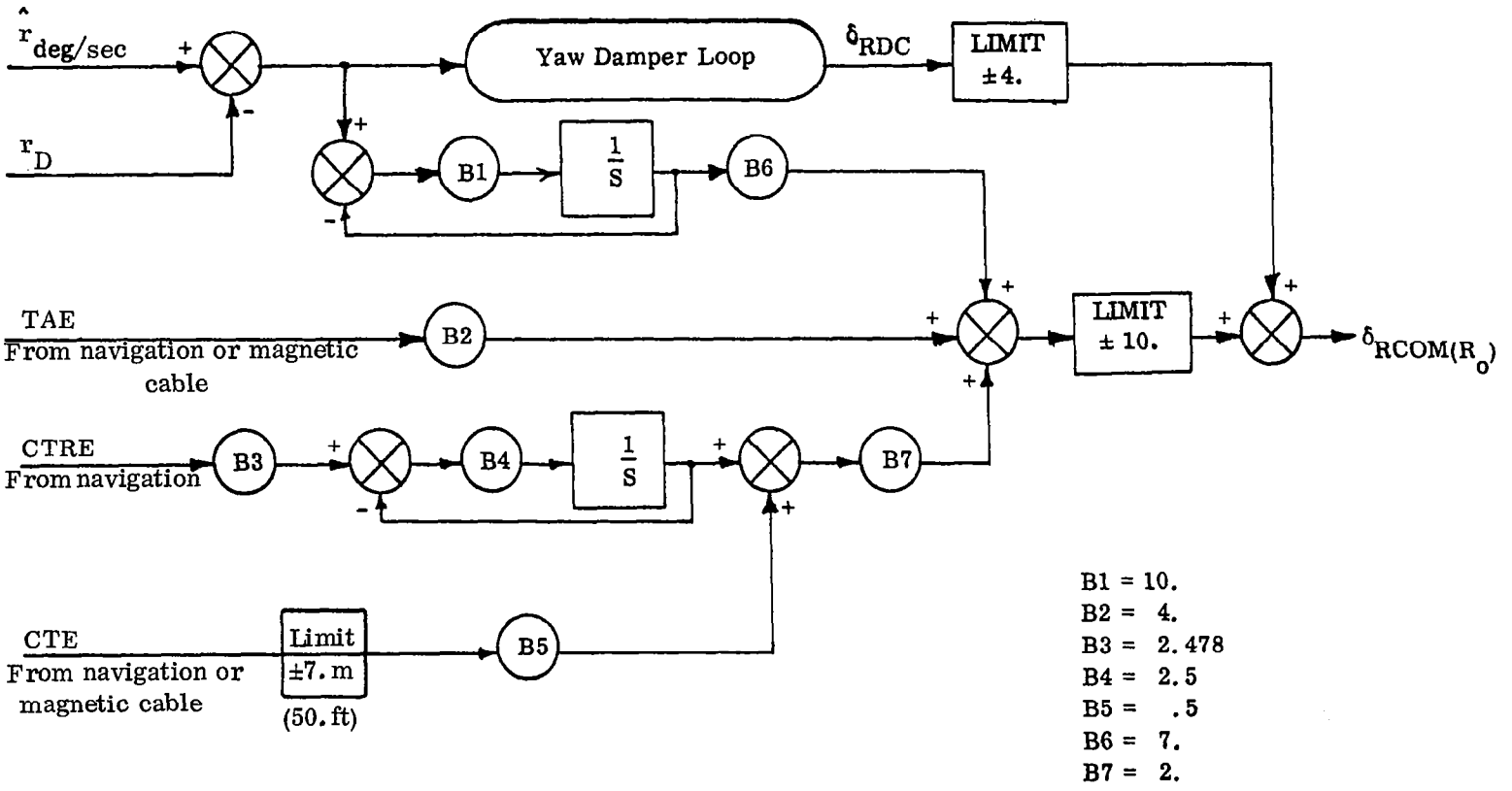

Figure 4. Rollout and Turnoff Steering Command

IV. DESCRIPTION OF THE NAVIGATION SYSTEM

The navigation system of the B737 consists of a stable platform which provides the rigid body inertial altitude and body angular rates. These are noisy and are subject to drift. Body mounted accelerometers provide a continuous measurement of the accelerations due to the external forces. These measurements are noisy and contain errors due to misalignment and scale factor errors.

Ref. (2) describes both a Kalman type filter and a constant gain complementary filter, either of which may be used to filter out the noisy measurements and provide for corrections so that the body mounted accelerometers may be integrated in an inertial reference frame to provide position, velocity acceleration, aircraft altitude and angular rates to the RNAV and displays. Fig. V is a block diagram of the Rollout and Turnoff Navigation and Guidance System.

Upon touchdown the major error source in the aircraft position is the down range position error due to the MLS range bias which cannot be removed by filtering. The range bias produces errors in the guidance signals which results in large tracking errors during the turn. This is illustrated in the first simulation run in Fig. VI. To eliminate this error source we recommend that the aircraft should receive a short radio blip signal as it passes a known position along the runway during rollout. By correcting the $\hat{x}$ coordinate to the known runway position, the offset problem disappears and good turnoffs may be realized.

The update equations are as follows:

Let the distance from the second way point to the blip location be BLIPX. Then

$$\text{XDIST} = \text{LSG}(1) - \text{BLIPX} \tag{33a}$$

$$\hat{X}(t_{BLIP}) = \text{XDIST} \tag{33b}$$

The use of a buried magnetic leader cable as described in Refs. (2) and (3) is under test at Langley Field and Wallops Island. Some results from these tests are given by Ref. 4. These tests indicate that while the use of sensors may provide a usable signal for the cross track error, the possibility of obtaining the track angle error (TAE) directly is in doubt. In any case, with the major source of error in the MLS measurement removed by the preceding BLIP technique, it should be possible to utilize MLS data to estimate TAE. Additional tests and simulation are recommended.

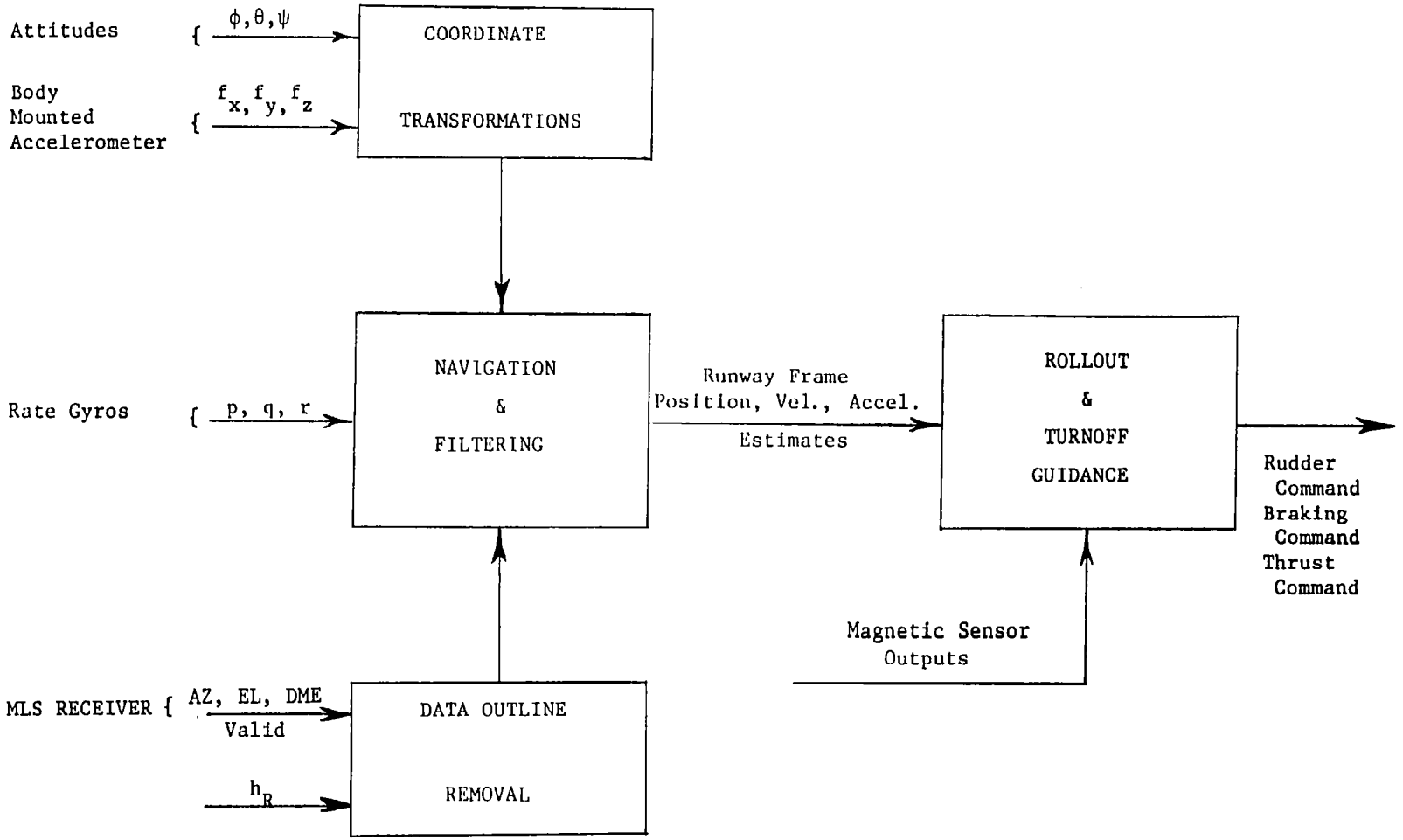

Figure 5. Rollout and Turnoff Navigation and Guidance System

V. SIMULATION RESULTS

This section contains the computer results of the simulation sensitivity study of the Langley TCV B737 aircraft in rollout, turnoff, and taxi. The runway geometry simulated was the Wallops Flight Center high speed exit on runway 22.

The factors affecting the study that were systematically varied are as follows:

1) The effect of MLS range bias error on lateral "stand off" in turns
2) The effect of aircraft speed in turns
3) The effect of winds, varying both the direction and magnitude
4) The effect of dry vs wet runways
5) The effect of magnetic sensor noise and bias
6) The effect of filtering methods on performance
7) The effect of turn radius
8) The effect of first exit distance on runway occupancy time
9) The effect of landing weights
10) The effect of parabolic vs circular turns on lateral acceleration in turns.

In order to illustrate the results of the study CALCOMP plots of the computer runs are shown in Figures 6 through 23. Table I contains a list of the parameters used in the simulation study for each plot.

Each simulation run consists of 12 plots of significant variables vs time. The items plotted are:

1) Thrust magnitude (Newtons)
2) Percent brake pressure command
3) Along track deceleration (g's)
4) Ground speed (m/sec)

TABLE I

ROLLOUT SENSITIVITY RUNS

FIG. #	RUNWAY COND.	TURN SPEED KN	TAXI SPEED KN	DIST. TO FIRST TURN (m)	WINDS SPEED/DIR	TURN RAD (m)	CIRCLE OR PARABOLA	WEIGHT (kg)	KALMAN COMP	NOISE AND BIAS
6	DRY	65	60	701.2	10/45°	548.6	C	40823.3	K	NO
7	"	65	60		0/0°	548.6	C	40823.3	K	NO
8	"	65	60		0/0°		C		C	NO
9	"	45	40				C		K	YES
10	"	65	60				C		K	
11	"	75	70				C		K	
12	"	45	40				C		C	
13	"	75	70				C		C	
14	"	75	70				PAR		K	
15	"	65	60				C		C	
16	WET	65	60			548.6	C		K	
17	DRY	65	60		0/0°	914.4	C		C	
18	"	65	60		10/45°	548.6	C		K	
19	"	65	60		15/0°		C		K	YES
20	"	65	60		0/0°	548.6	C	40823.3	K	Excessive Noise
21	"	65	60		0/0°	548.6	C	31751.5	C	YES
22	DRY	65	60	1097.3	0/0°	548.6	C	40823.3	C	YES

5) Yaw (Degrees)

6) Cross track error (meters)

7) Nose wheel steering command (degrees)

8) Error in estimates of runway position coordinates for the navigation filter used in simulation run

9) Error in estimates of velocity components in the runway coordinate frame for the navigation filter used in the simulation run

10) Track angle error (degrees)

11) Cross track velocity error (m/sec)

12) Cross track acceleration (g's)

A brief discussion of the significant features of Figures 6 through 21 follow.

Figure 6 contains a typical automated rollout and turnoff when no information is available to the navigation system to eliminate the MLS range bias in the DME signal. The rollout is completed in an acceptable manner, however, the cross track error (Plot #6, Figure 6) shows a fixed "stand off" resulting from the down track error in position (Plot #8, Figure 6) settling into a cross track error in the turn. The fix for this effect is to give the navigation system a more accurate along track position measurement early in the rollout so that the system knows where it is relative to the beginning of the turn. Figure 7 and all subsequent figures contain this blip information and a readjustment can be noted in x-position error (Plot #8, Figs. 6 - 21) shortly after touchdown. It may be noted that the large "stand off" error in cross track is no longer present in these figures.

Figures 7 and 8 illustrate the performance of both the Kalman and complementary filters as navigation aids when no noise or bias is present in the magnetic leader cable. Response to cable noise and bias due to conducting reenforcing rods in the runway pavement construction is mainly present in the nose wheel steering command channel (Plot #7, Figs. 9 - 19). In contrast to Figs. 7 and 8 one may examine Fig. 20 in which excessive noise drives a

nose wheel command chatter. The aircraft is moving too rapidly to follow the nose wheel motion, however the effect is to produce an unacceptable nose wheel response. The results of the tests in Ref. 4 would indicate that the yaw deviation signal coming from the magnetic cable sensor may have to be eliminated and possibly replaced by information from the INS and pre-stored information regarding the runway center heading. Additional study will be required to solve this problem.

Figures 9, 10, 11, 12, and 13 illustrate the performance of the automated rollout and turnoff as a function of turn speed using either Kalman or the complementary filters. The main features to be noted are that the cross track acceleration (Plot 12, Figs. 11 and 13) for a 75 knot turn produces a maximum lateral acceleration of 0.3 g's which borders on the uncomfortable. This is due to an S shape reversal in the turnoff pattern (Figure 2). An acceptable sustained maximum lateral acceleration is on the order of 0.2 g's during a steady turn. Figure 14 illustrates the effect of attempting to alleviate the severity of the turn rate onset using a "centered" parabolic turn. It is evident that no significant improvement is forthcoming from this technique. The improvement was small because the "centered" parabola path did not differ significantly from the circular path for this 30^{o} turn. It is possible that by "easing in" the turn signal in the guidance law loop may help to eliminate this effect. Additional work remains to be done in this area if 75 knot turns are to be mandated for runway occupancy reduction.

It is significant to note that turnoffs at speeds of 45 and 65 knots may be executed in this automated mode. It is questionable whether a manual operated system could perform as well at these speeds.

Figure 22 illustrates the effect of turnoff distance on runway occupancy. Contrasting Fig. 10 and 22 both of which call for the same turnoff speed at different turnoff distances (Figure 22 turnoff distance is 1300 feet longer) show almost identical behavior except that there is practically no braking for the longer turnoff distance since the reverse thrust is able to achieve the turn speed

at the proper turn distance without additional braking. The runway occupancy increases from 15 seconds for the shorter turnoff runway as compared with 20 seconds for the longer turnoff runway in Fig. 22.

The effect of wet runways is illustrated in Fig. 16. This case is to be compared with Fig. 9 both of which call for a turn speed of 45 knots. The wet runway case cannot achieve the deceleration in time to make the turn at first turn opportunity since the ground speed exceeds the hydroplane speed and no braking is permitted. By calling for the next turn opportunity, the wet runway case is able to achieve the turn speed at just under 25 seconds and is able to execute a safe exit at 45 knots.

Figure 18 illustrates the effect of turn radius on the cross track acceleration. By contrasting Fig. 17 with Figure 10 we obtain the expected results. The sustained lateral acceleration in the steady 65 knot turn at a radius of 548.6m is reduced from .2 g's to .11 g's at 65 knots and 914.4m radius.

The effect of winds in varying directions is illustrated in Figures 18 and 19. These runs are to be contrasted with Fig. 10. All three call for a turn speed of 65 knots. The effect of winds is to increase the maximum cross track error from 4 meters for the case of no winds to 6 meters for 10. knot winds. The cause of the overshoot is that winds provide for additional yaw rate as the aircraft heading changes making it more difficult for the rollout control law to maintain the desired heading in a turn. It is possible that feeding in information on wind direction could provide for a better control in cross track error during the turn in a wind condition. Additional study is required in this area.

Figure 21 shows the effect of aircraft weight. The major effect is to reduce the braking required for deceleration, since the reduced weight (40823.3 kg in Fig. 10 is reduced to 31751.5kg in Fig. 21) permits the reverse thrust to achieve the turn speed of 65 knots without much brake assist.

VI. CONCLUSIONS AND RECOMMENDATIONS

In general, it is concluded that runway occupation time can be significantly reduced by use of automated rollout and turnoff capability. The aircraft can be clear of the runway within 20 seconds for dry runways and 30 seconds for wet runways. It is further concluded that turns of 33.4 m/s (54 knots) at 548.8 in. (1800 ft) radii or larger can be automatically and safely achieved.

It is recommended that rollout and turnoff guidance laws to reduce cross track errors due to winds be investigated.

It is also recommended that "slow in" logic be investigated to ease the onset of turn acceleration.

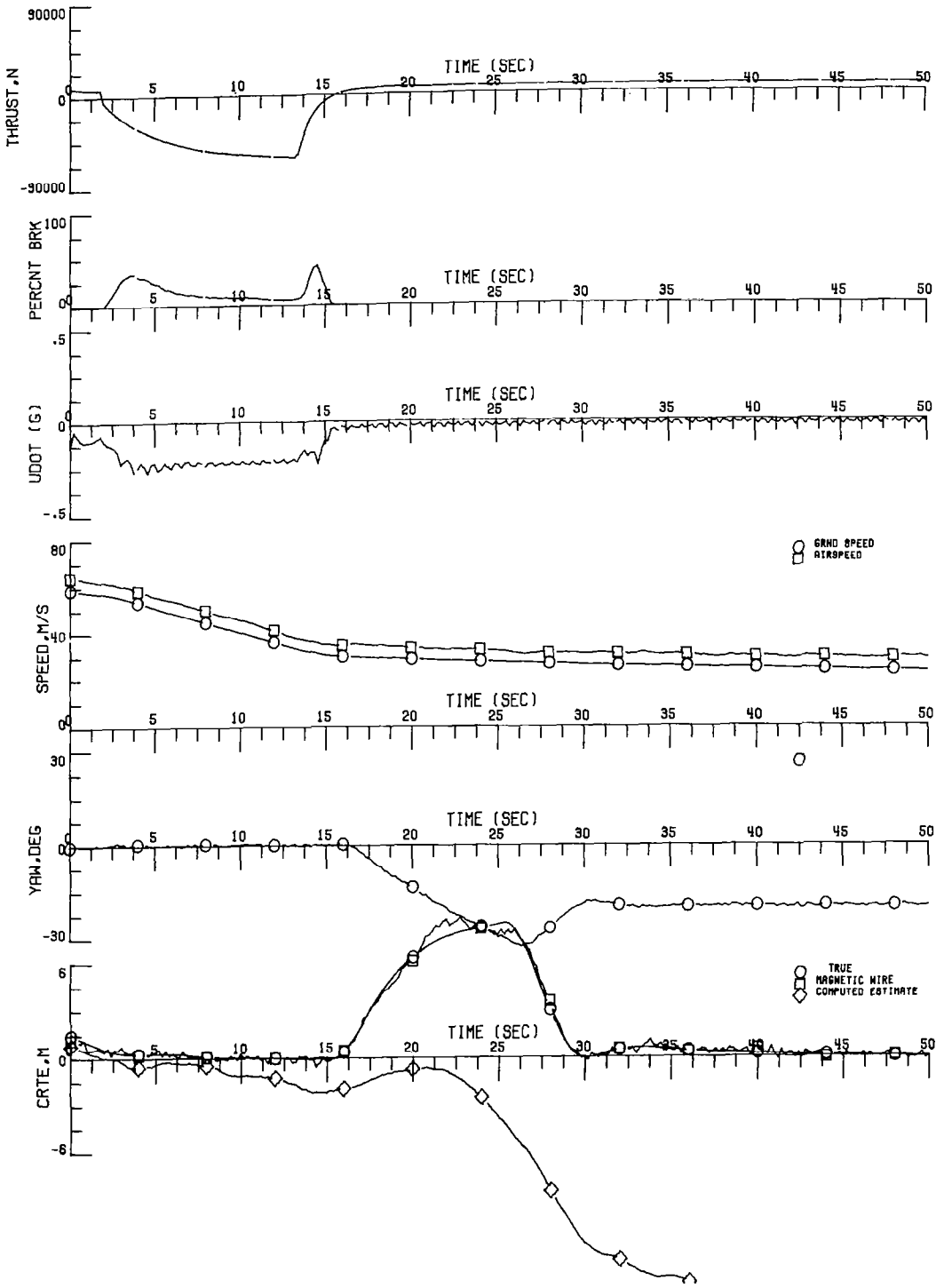

Figure 6. Rollout and Turnoff Without Blip Sensor on Dry Runway

Note: Standoff in Plot #6 CRTE

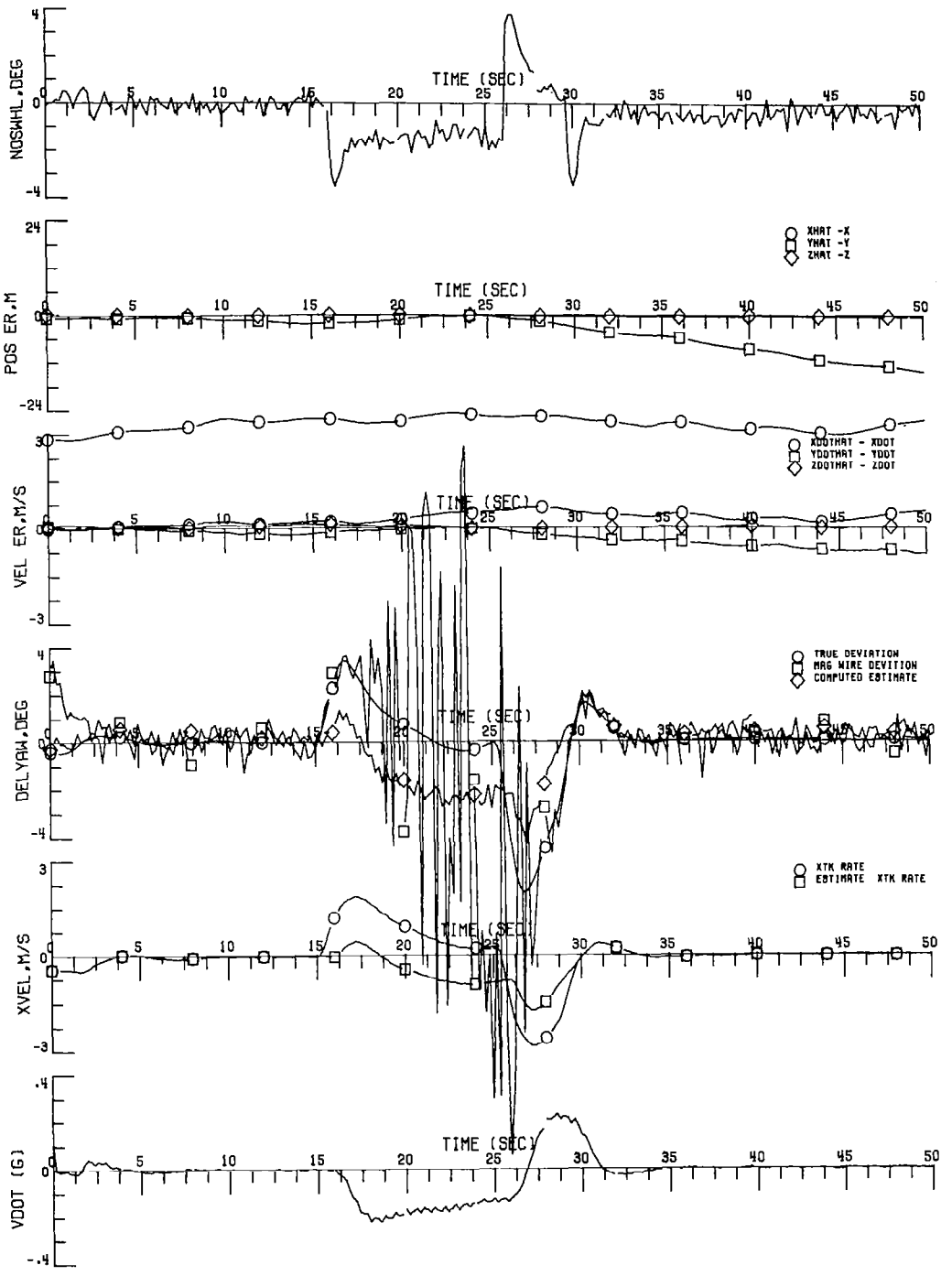

Figure 6. (Concluded)

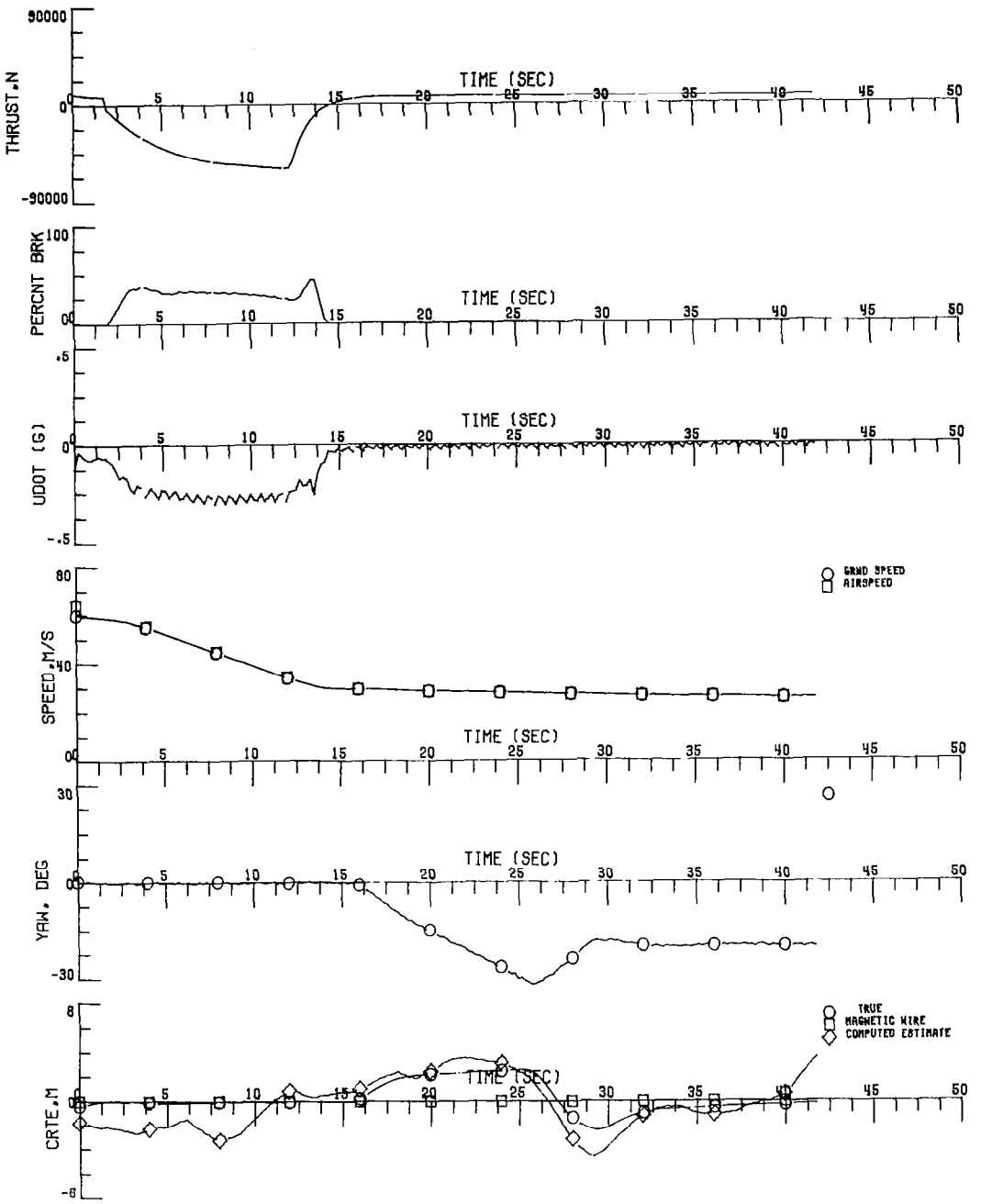

Figure 7. Rollout and Turnoff With Blip Sensor on Dry Runway - No Noise

Turn Speed = 65 knots
Taxi Speed = 60 knots
No Winds
Turn Radius = 548.6 m
Landing Wt. = 40823.3 kg
Kalman Filter Used

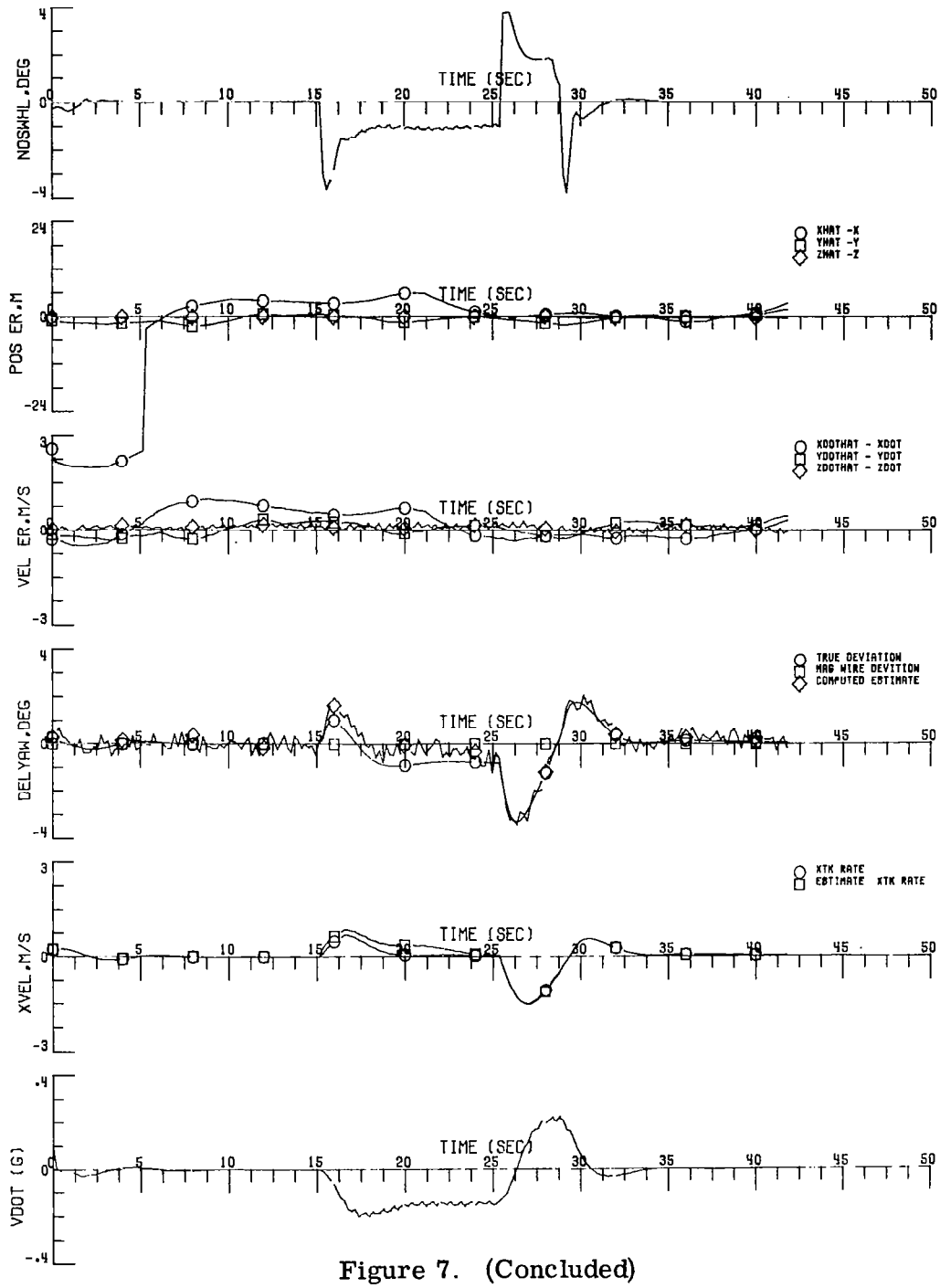

Figure 7. (Concluded)

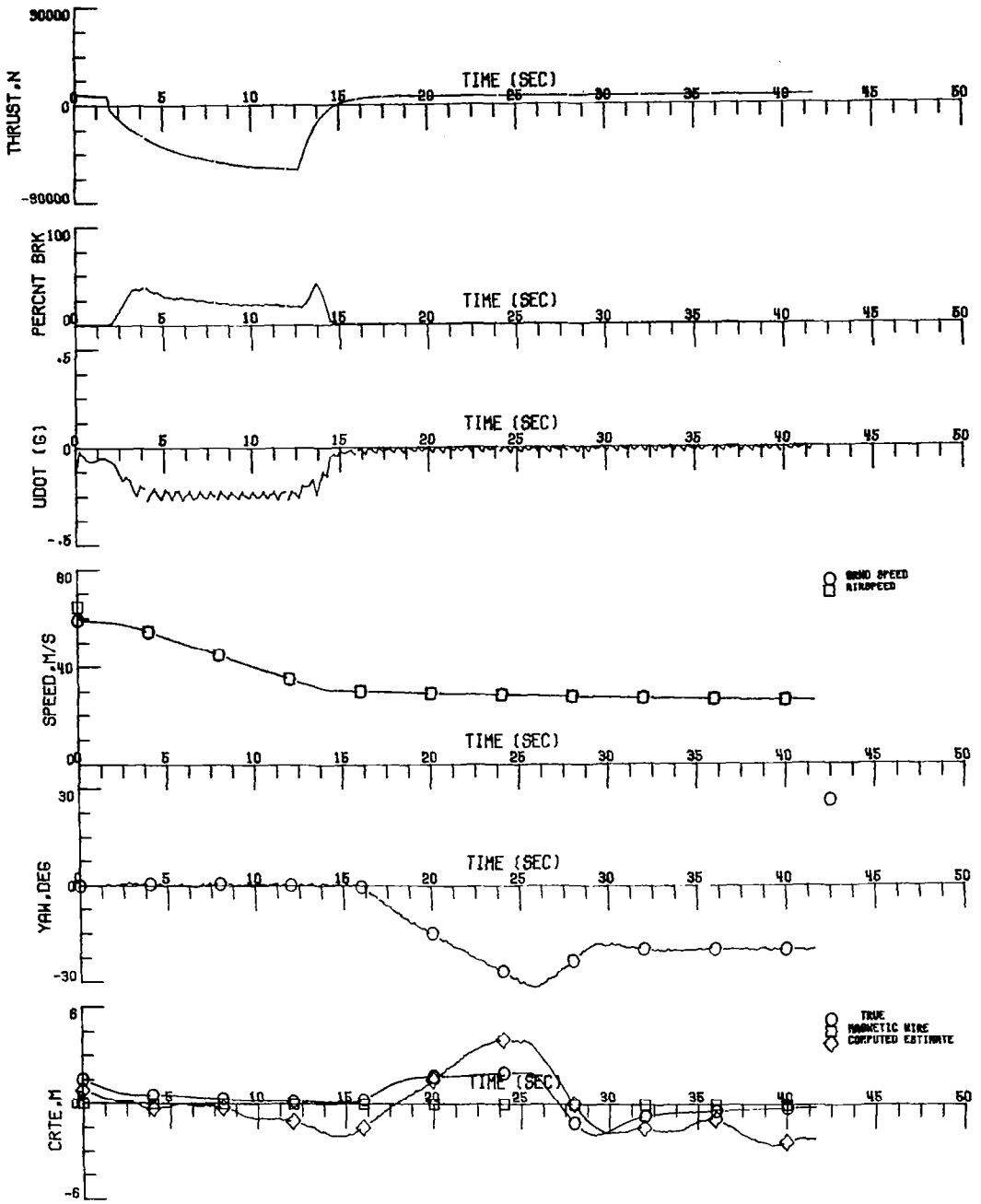

Figure 8. Rollout and Turnoff With Blip Sensor on Dry Runway - No Noise

Turn Speed = 65 knots
Taxi Speed = 60 knots
No Winds
Turn Radius = 548.6 m
Landing Wt. = 40823.3 kg
Complementary Filter Used

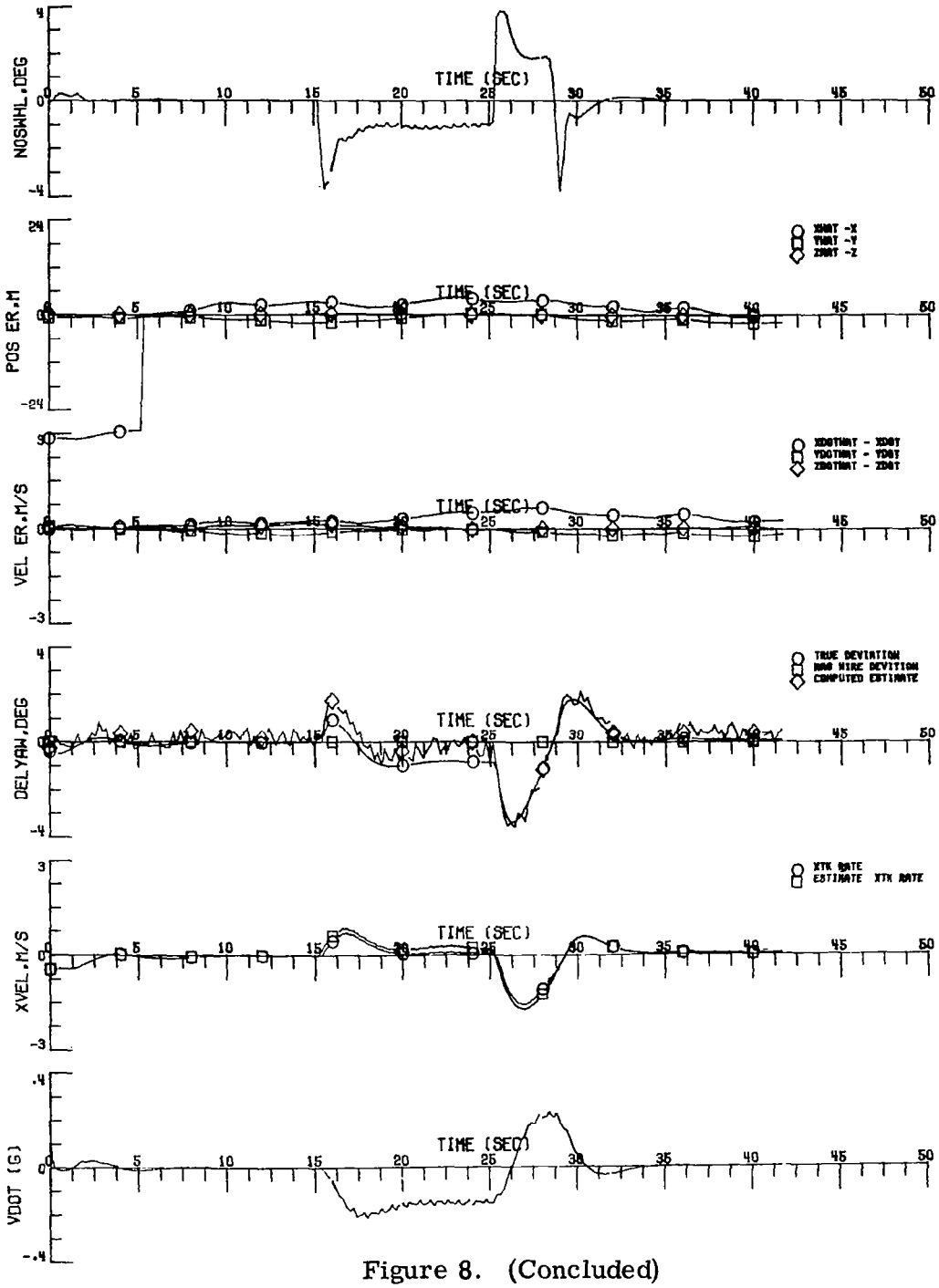

Figure 8. (Concluded)

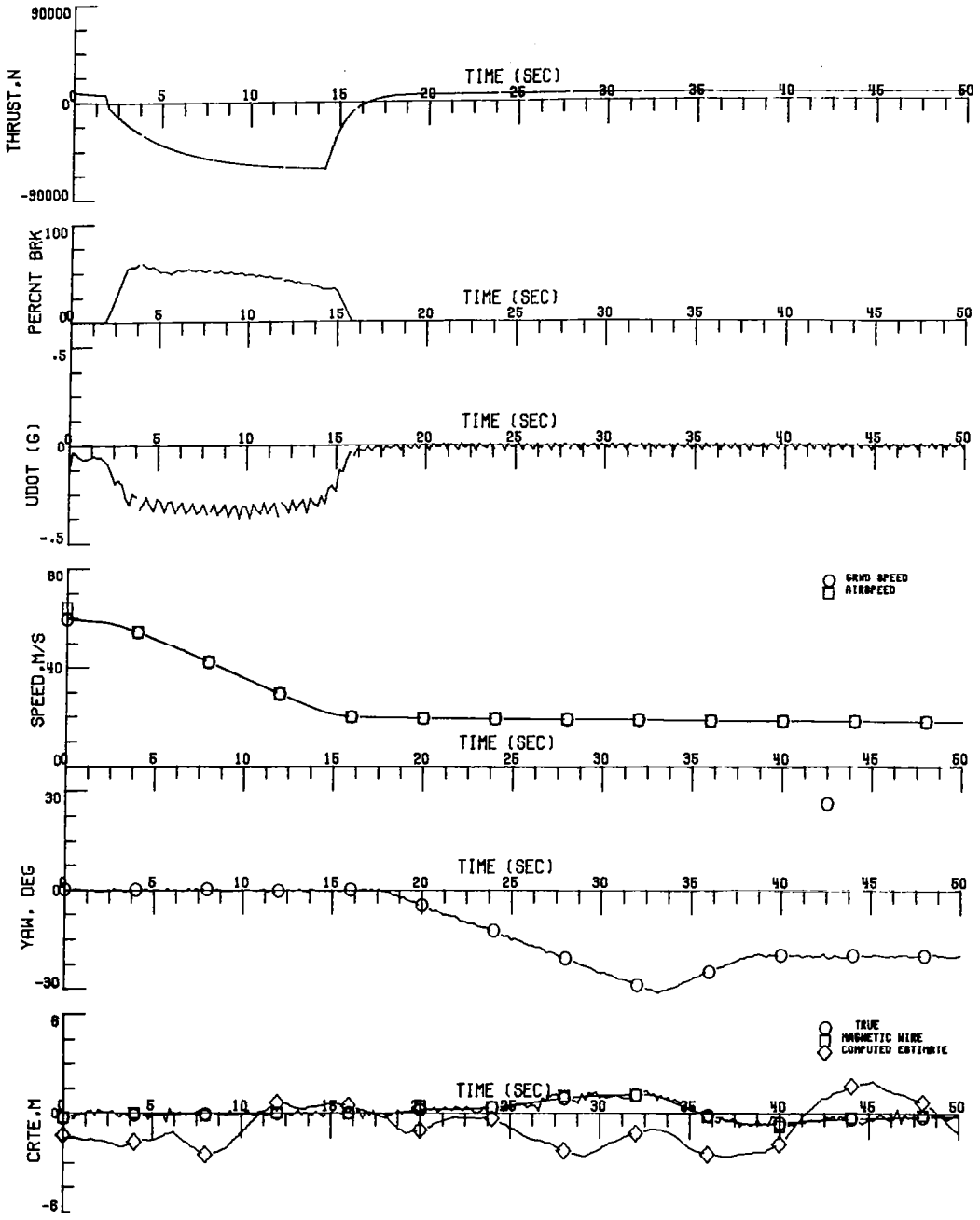

Figure 9. Rollout and Turnoff on Dry Runway – Noise and Bias Acting

Turn Speed = 45 knots
Taxi Speed = 40 knots
No Winds
Turn Radius = 548.6 m
Landing Wt. = 40823.3 kg
Kalman Filter Used

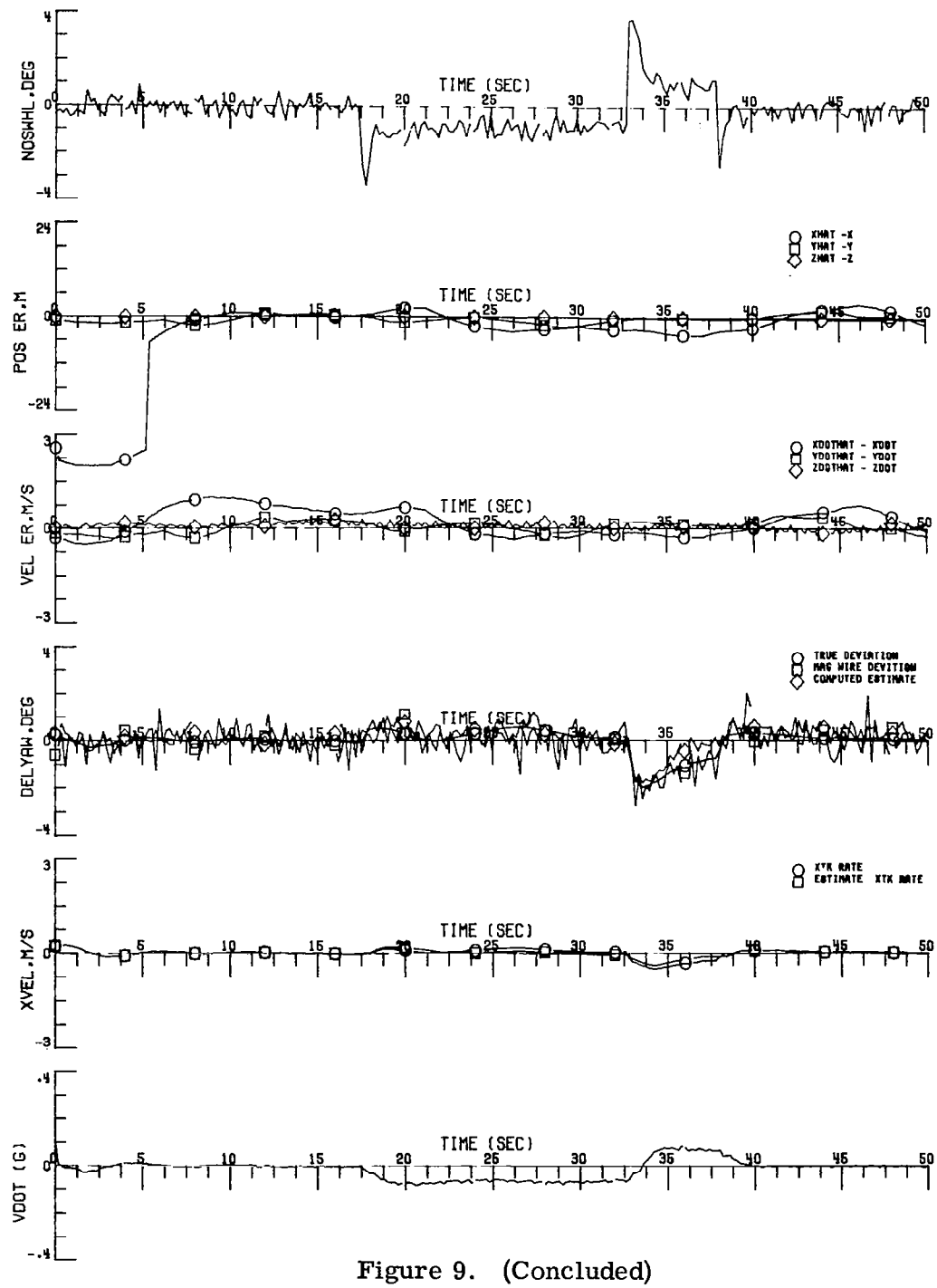

Figure 9. (Concluded)

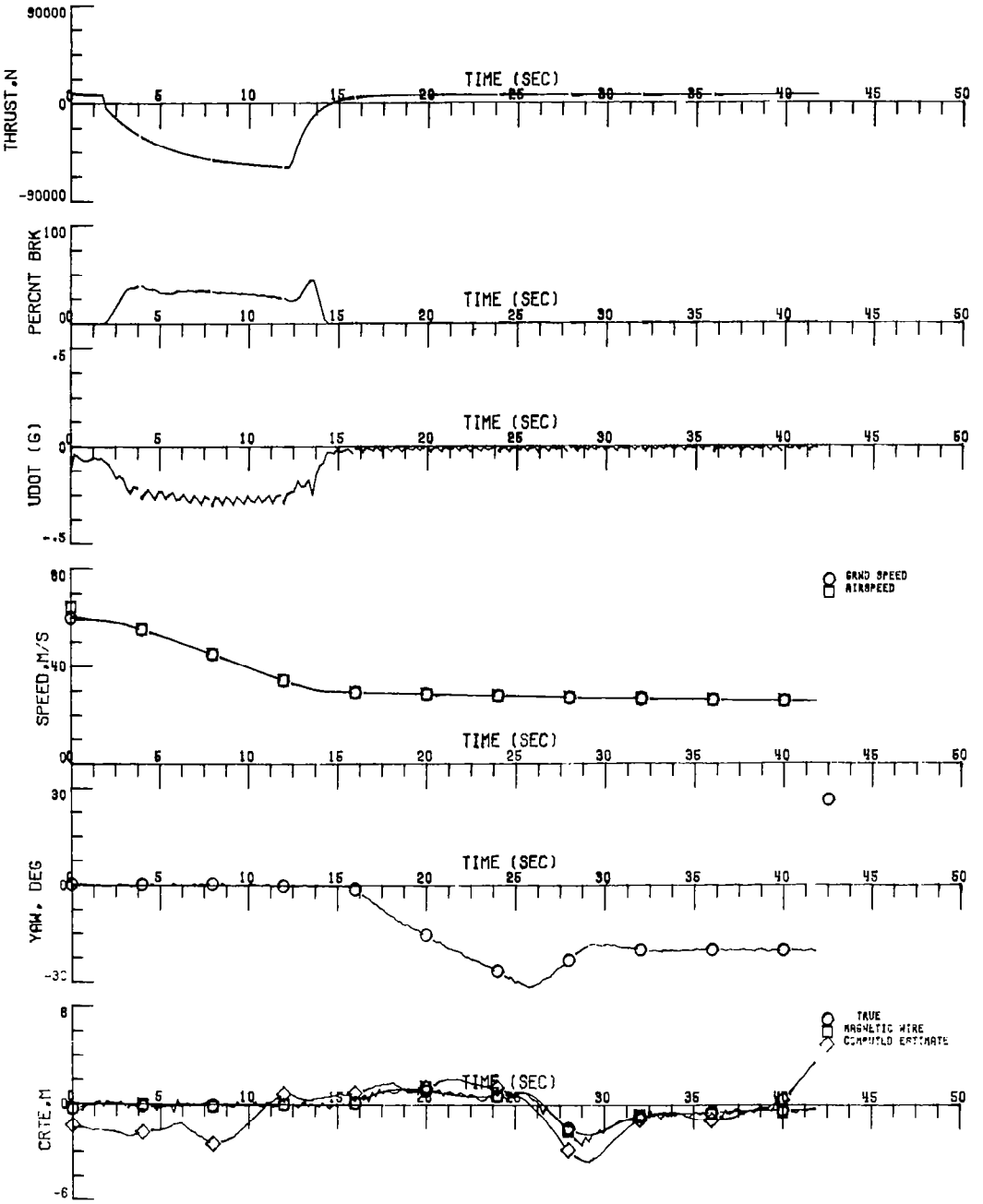

Figure 10. Rollout and Turnoff on Dry Runway - Noise and Bias Acting

Turn Speed = 65 knots
Taxi Speed = 60 knots
No Winds
Turn Radius = 548.6 m
Landing Wt. = 40823.3 kg
Kalman Filter Used

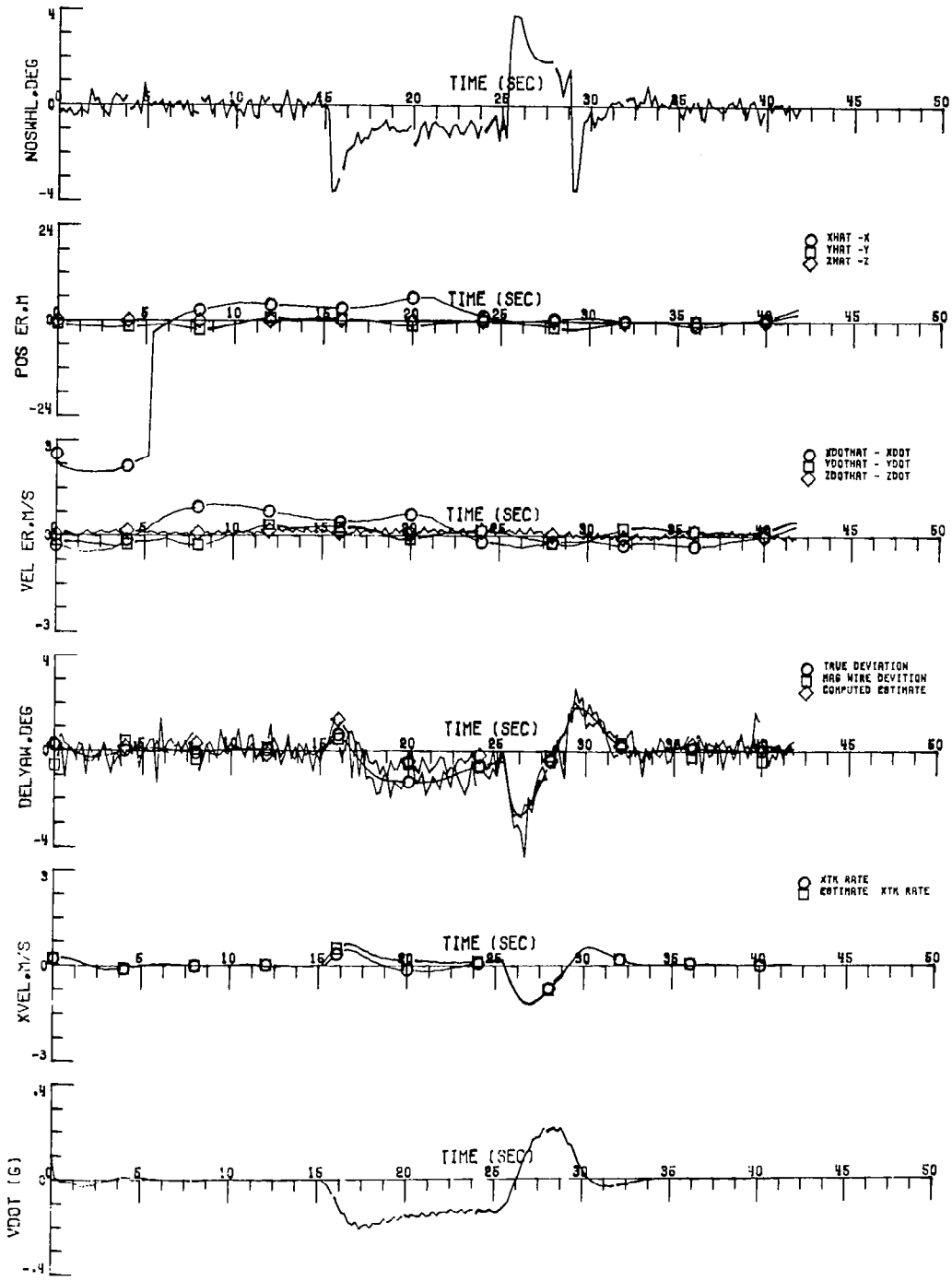

Figure 10. (Concluded)

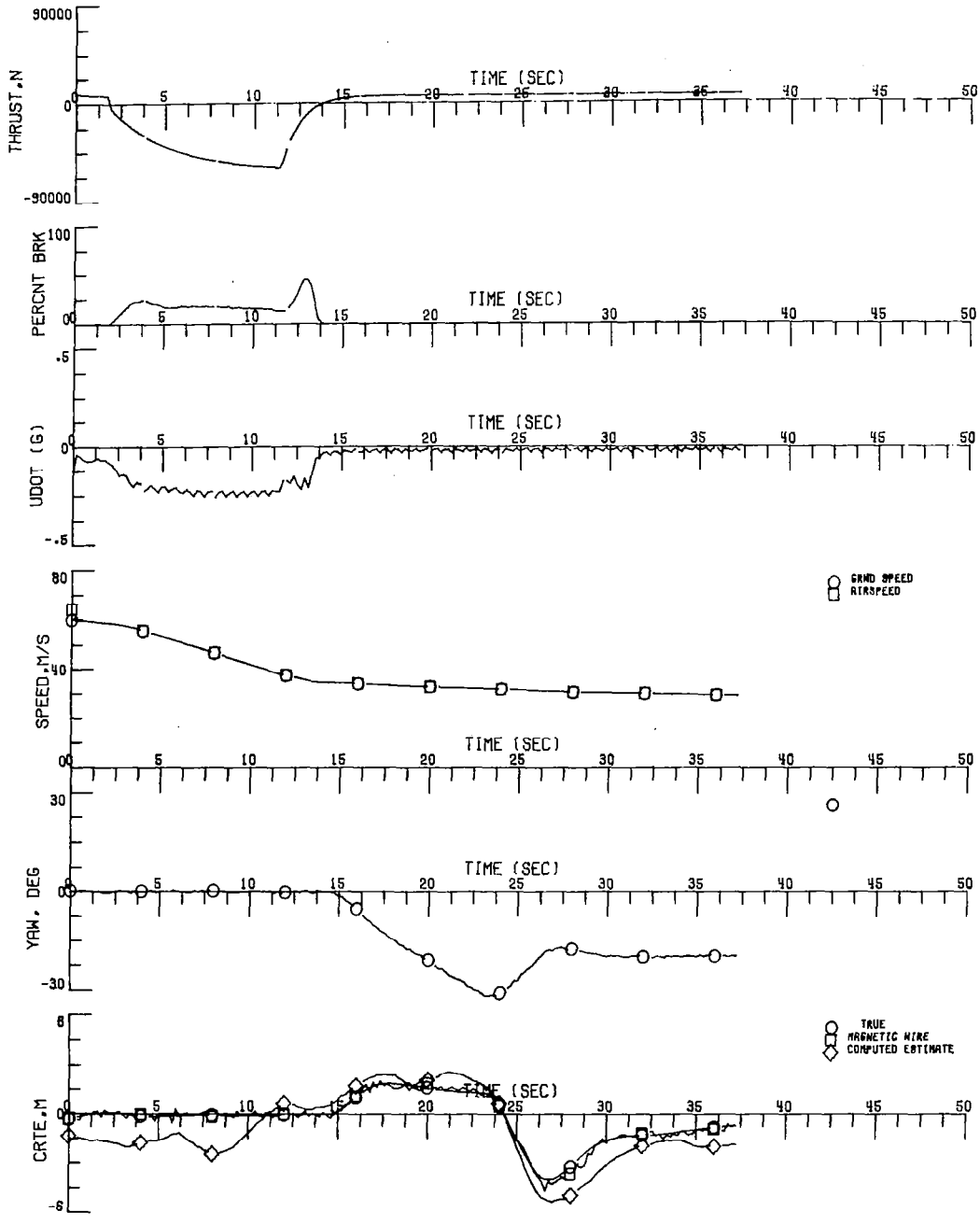

Figure 11. Rollout and Turnoff on Dry Runway - Noise and Bias Acting

Turn Speed = 75 knots
Taxi Speed = 70 knots
No Winds
Turn Radius = 548.6 m
Landing Wt. = 40823.3 kg
Kalman Filter Used

Note: High Lateral Acceleration in Plot #12

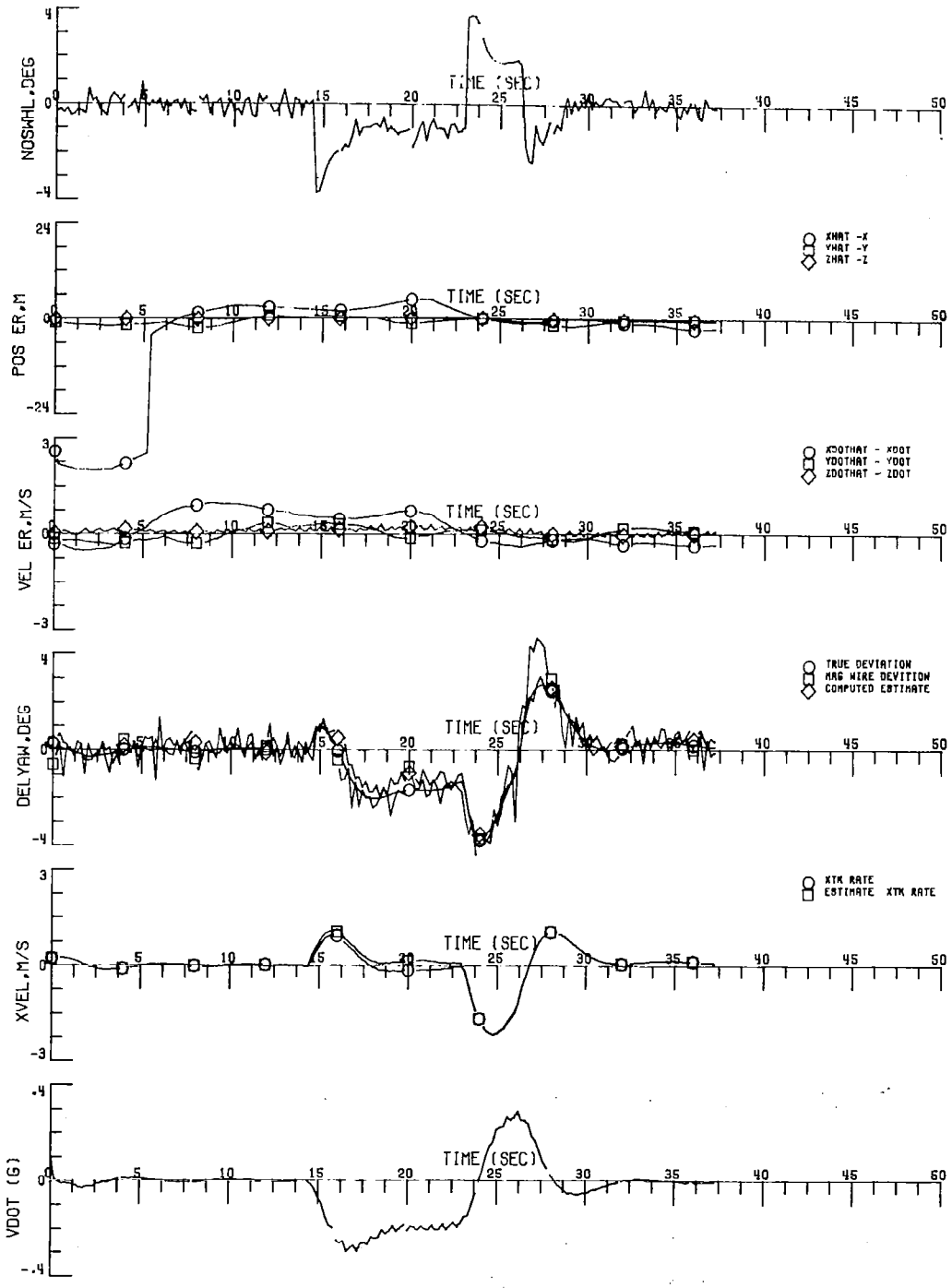

Figure 11. (Concluded)

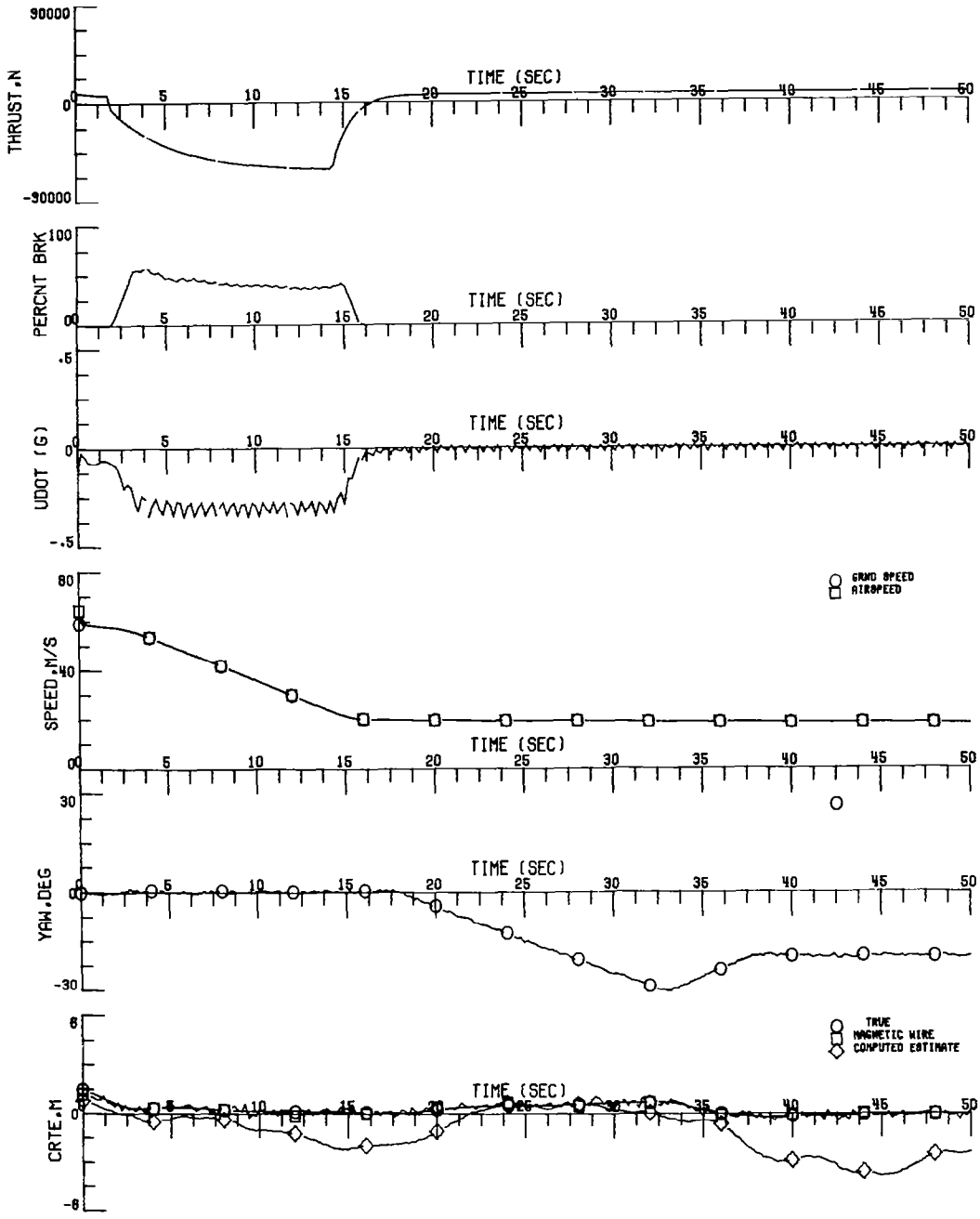

Figure 12. Rollout and Turnoff on Dry Runway - Noise and Bias Acting

Turn Speed = 45 knots
Taxi Speed = 40 knots
No Winds
Turn Radius = 548.6 m
Landing Wt. = 40823.3 kg
Complementary Filter Used

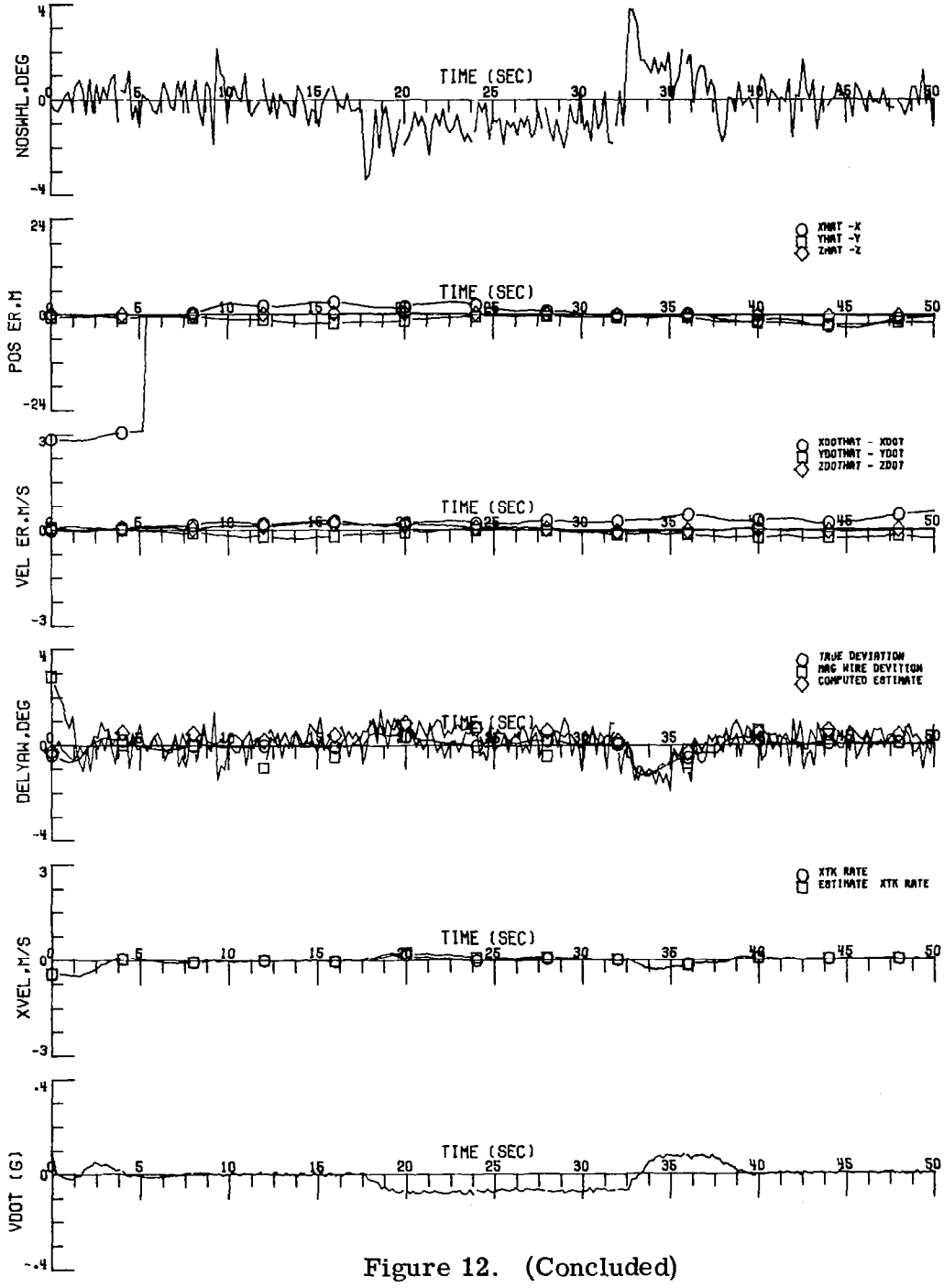

Figure 12. (Concluded)

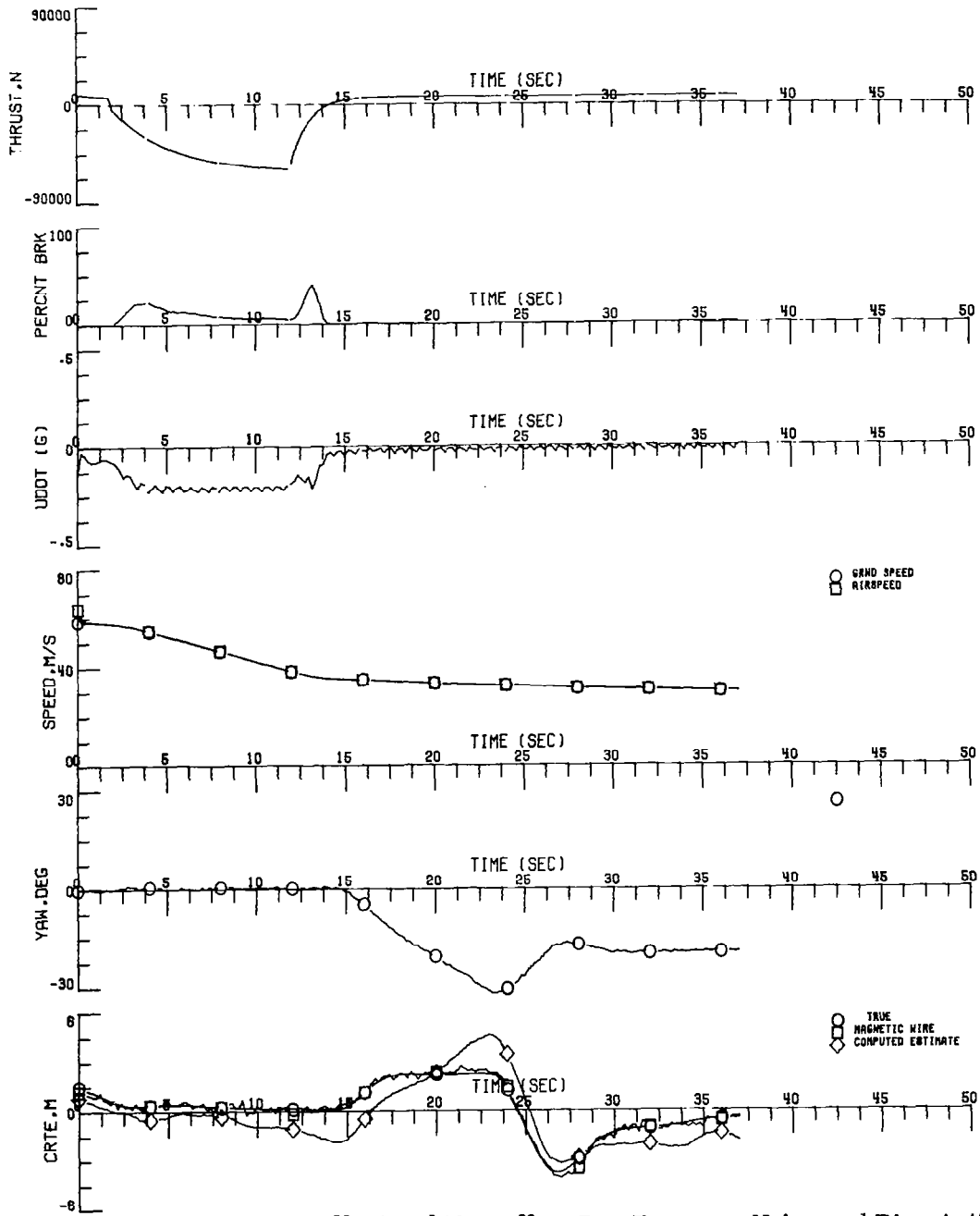

Figure 13. Rollout and Turnoff on Dry Runway - Noise and Bias Acting

Turn Speed = 75 knots
Taxi Speed = 70 knots
No Winds
Turn Radius = 548.6 m
Landing Wt. = 40823.3 kg
Complementary Filter Used

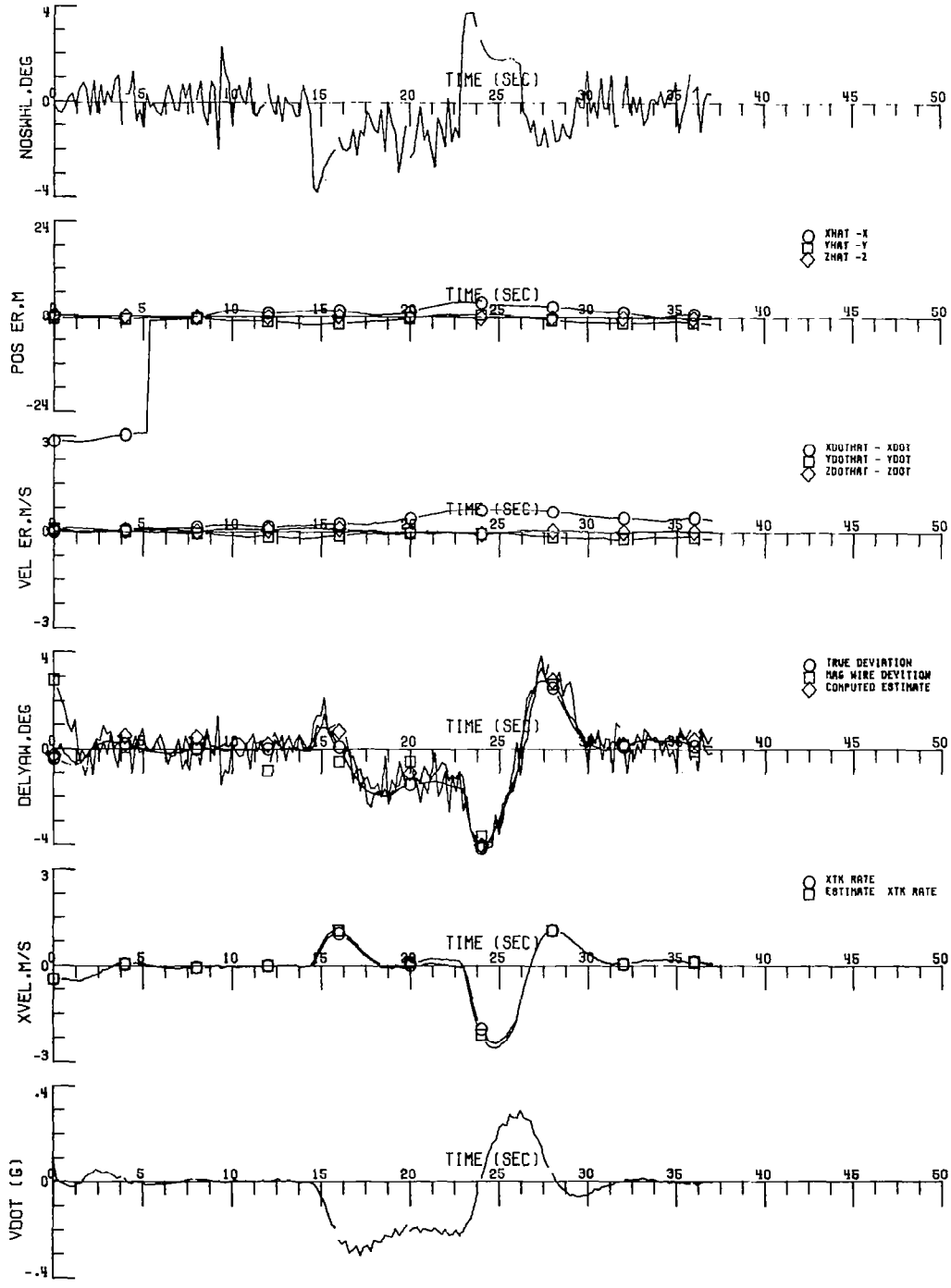

Figure 13. (Concluded)

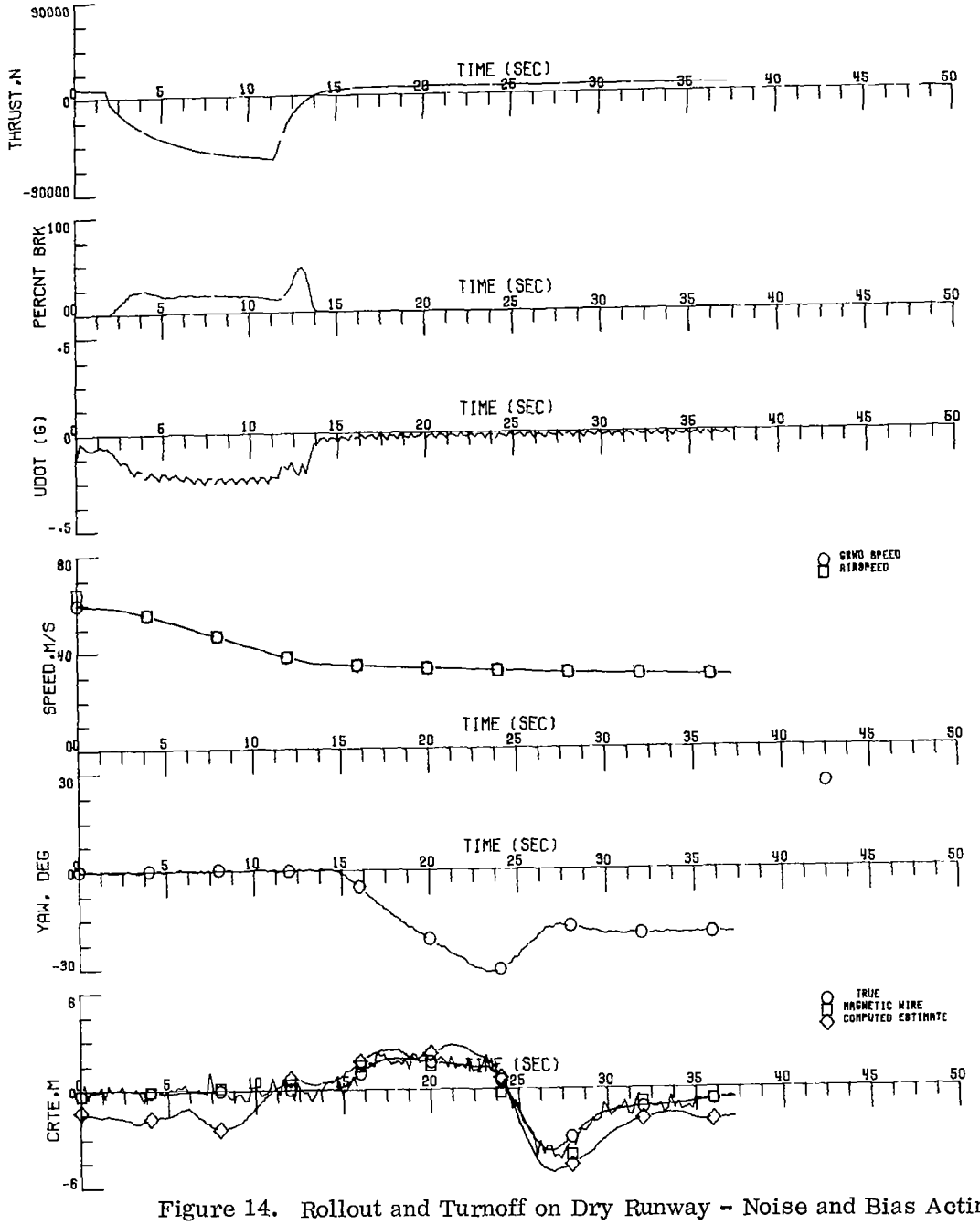

Figure 14. Rollout and Turnoff on Dry Runway - Noise and Bias Acting

Turn Speed = 75 knots
Taxi Speed = 70 knots
No Winds
Turn Radius = 548.6 m
Parabolic Turn
Landing Wt. = 40823.3 kg
Kalman Filter Used

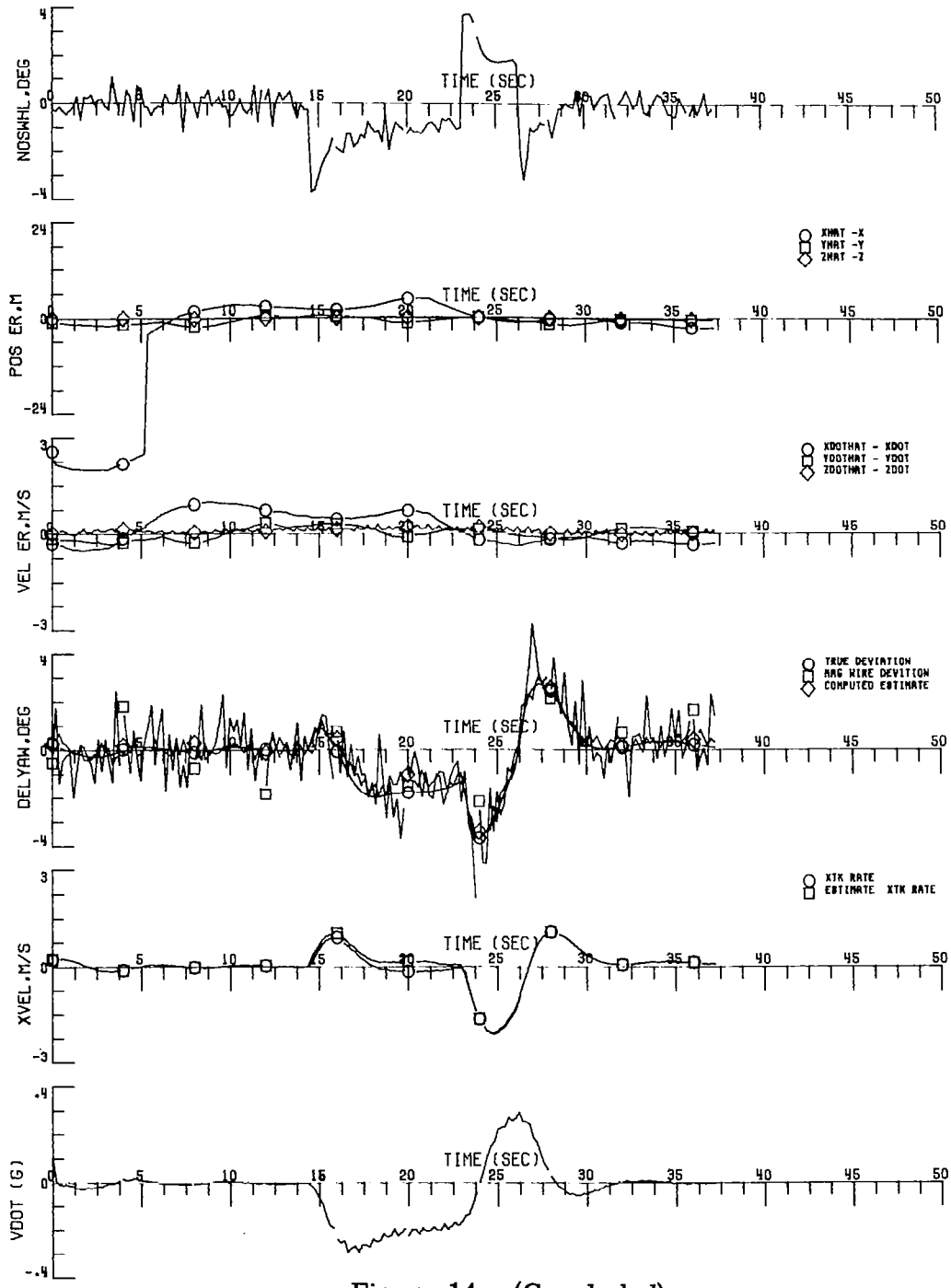

Figure 14. (Concluded)

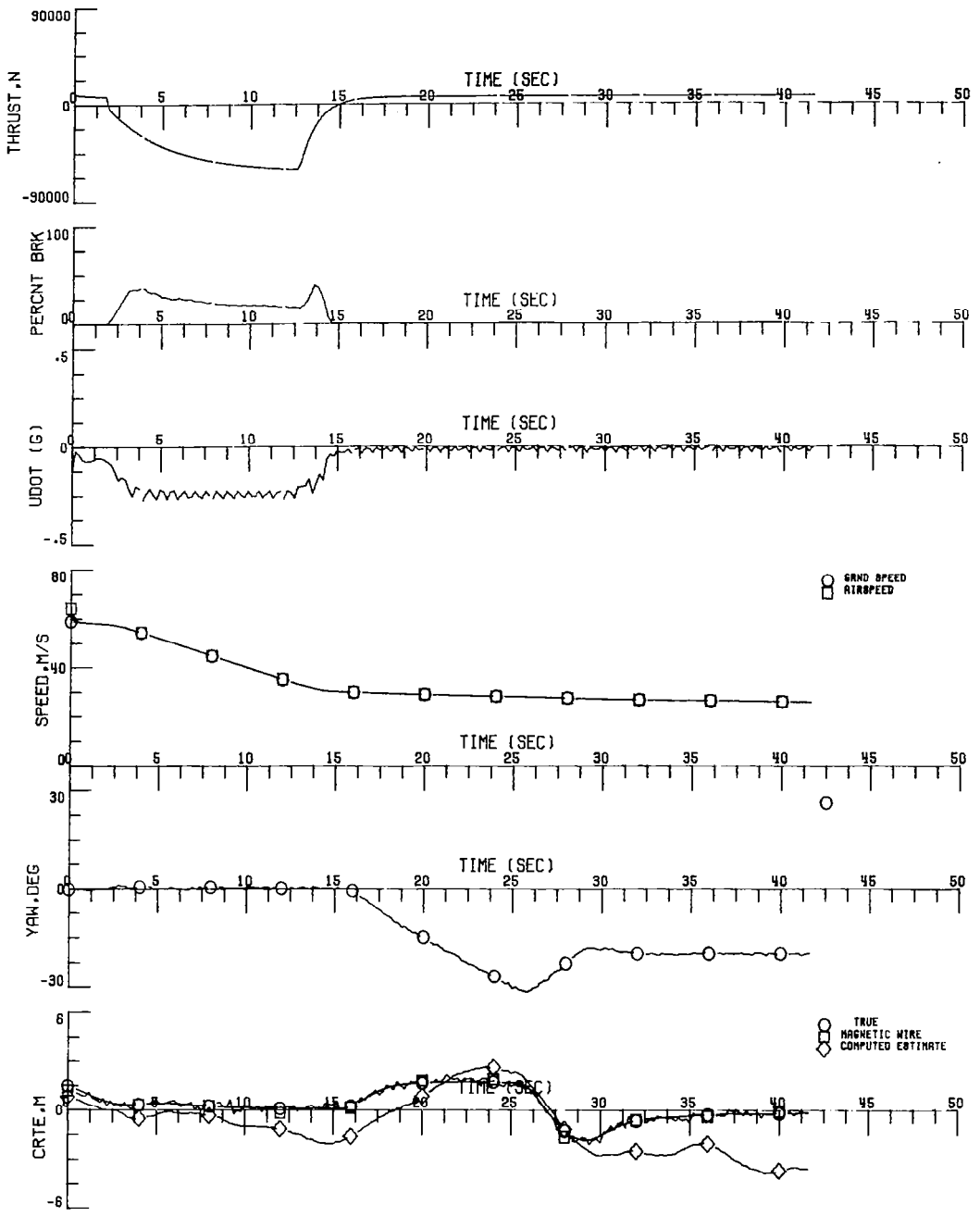

Figure 15. Rollout and Turnoff on Dry Runway - Noise and Bias Acting

Turn Speed = 65 knots
Taxi Speed = 60 knots
No Winds
Turn Radius = 548.6 m
Landing Wt. = 40823.3 kg
Complementary Filter Used

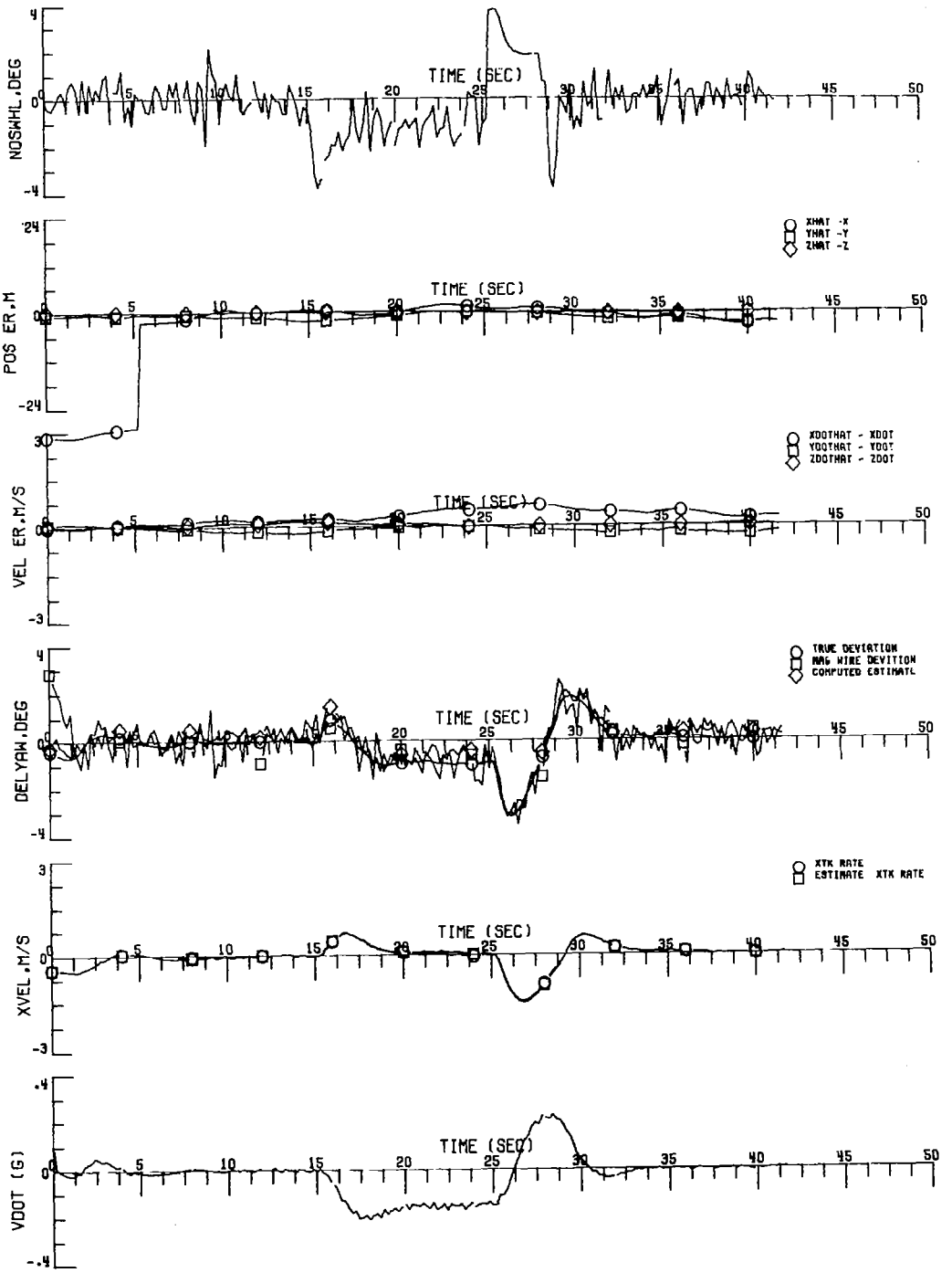

Figure 15. (Concluded)

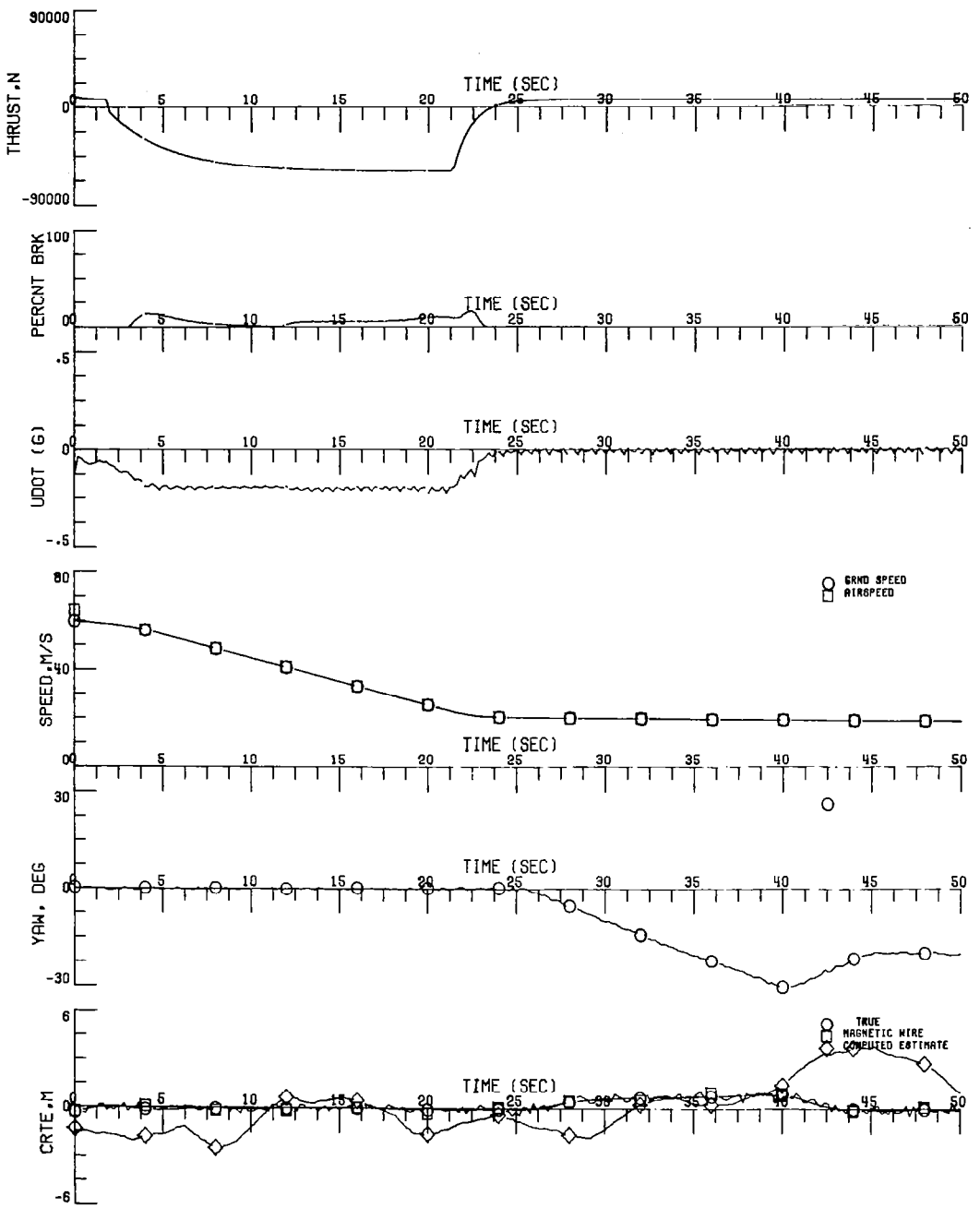

Figure 16. Rollout and Turnoff on Wet Runway – Noise and Bias Acting

Turn Speed = 65 knots
Taxi Speed = 60 knots
No Winds
Turn Radius = 548.6 m
Landing Wt. = 40823.3 kg
Kalman Filter Used

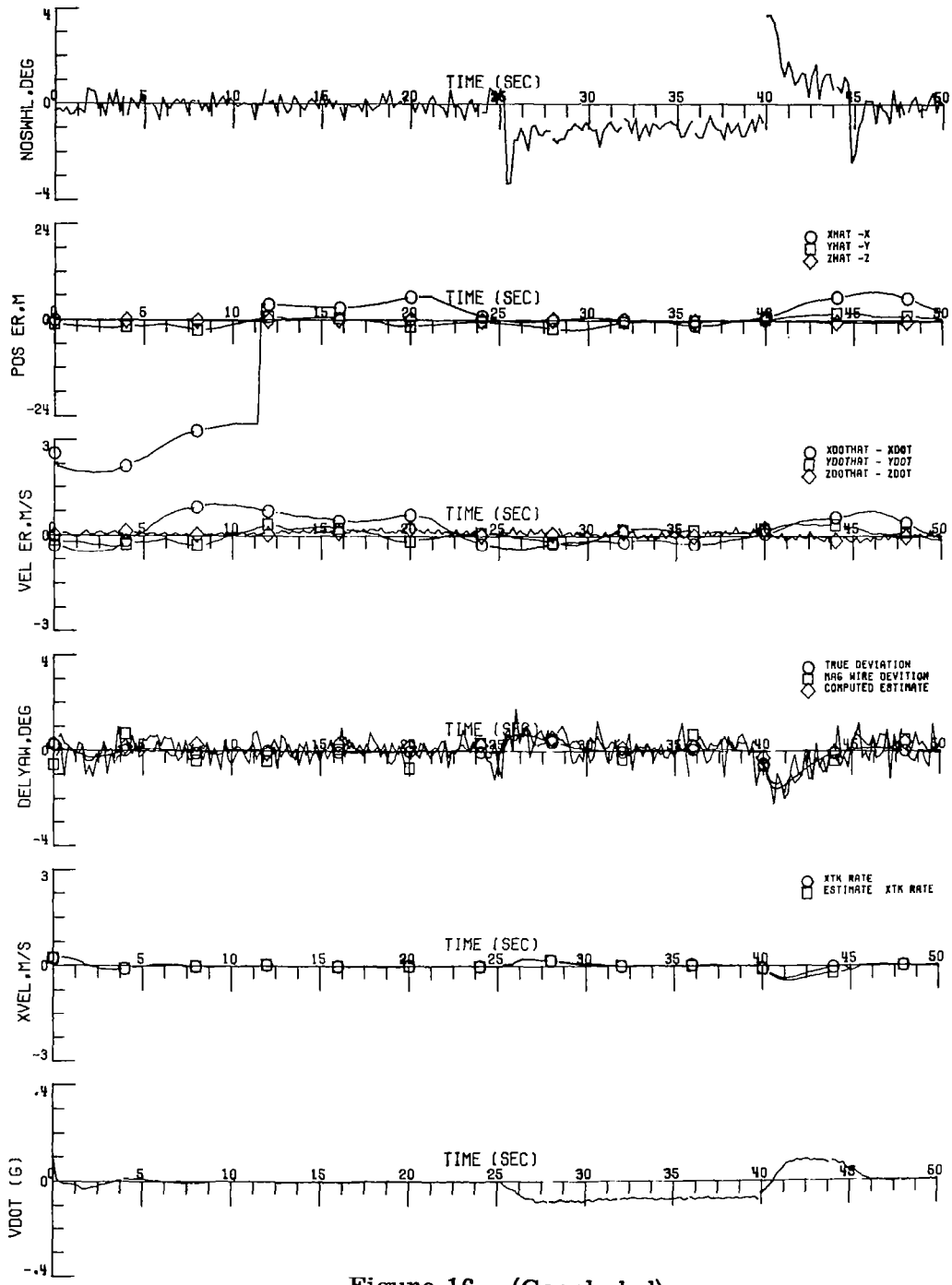

Figure 16. (Concluded)

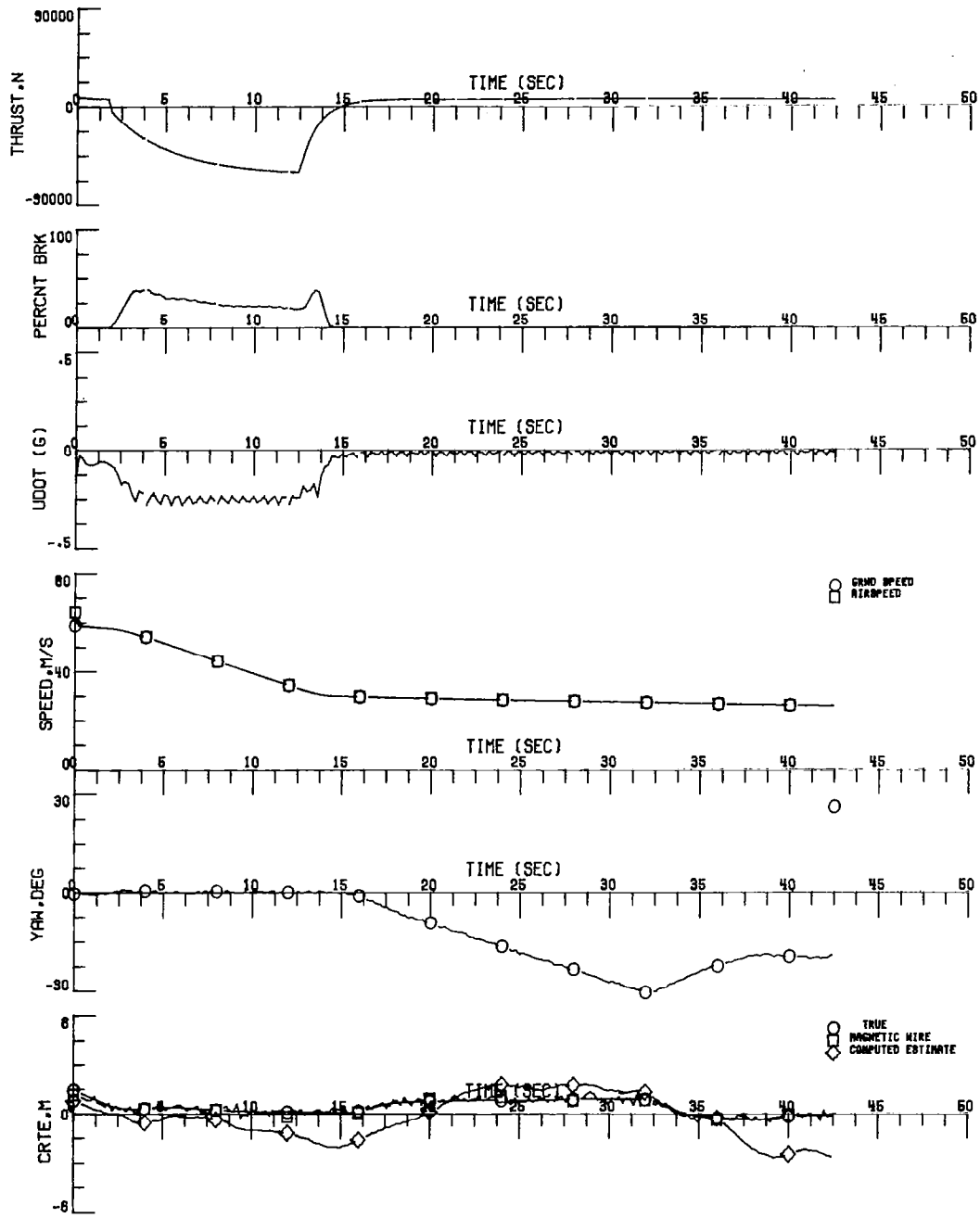

Figure 17. Rollout and Turnoff on Dry Runway - Noise and Bias Acting

Turn Speed = 65 knots
Taxi Speed = 60 knots
No Winds
Turn Radius = 914.4 m
Landing Wt. = 40823.3 kg
Complementary Filter Used

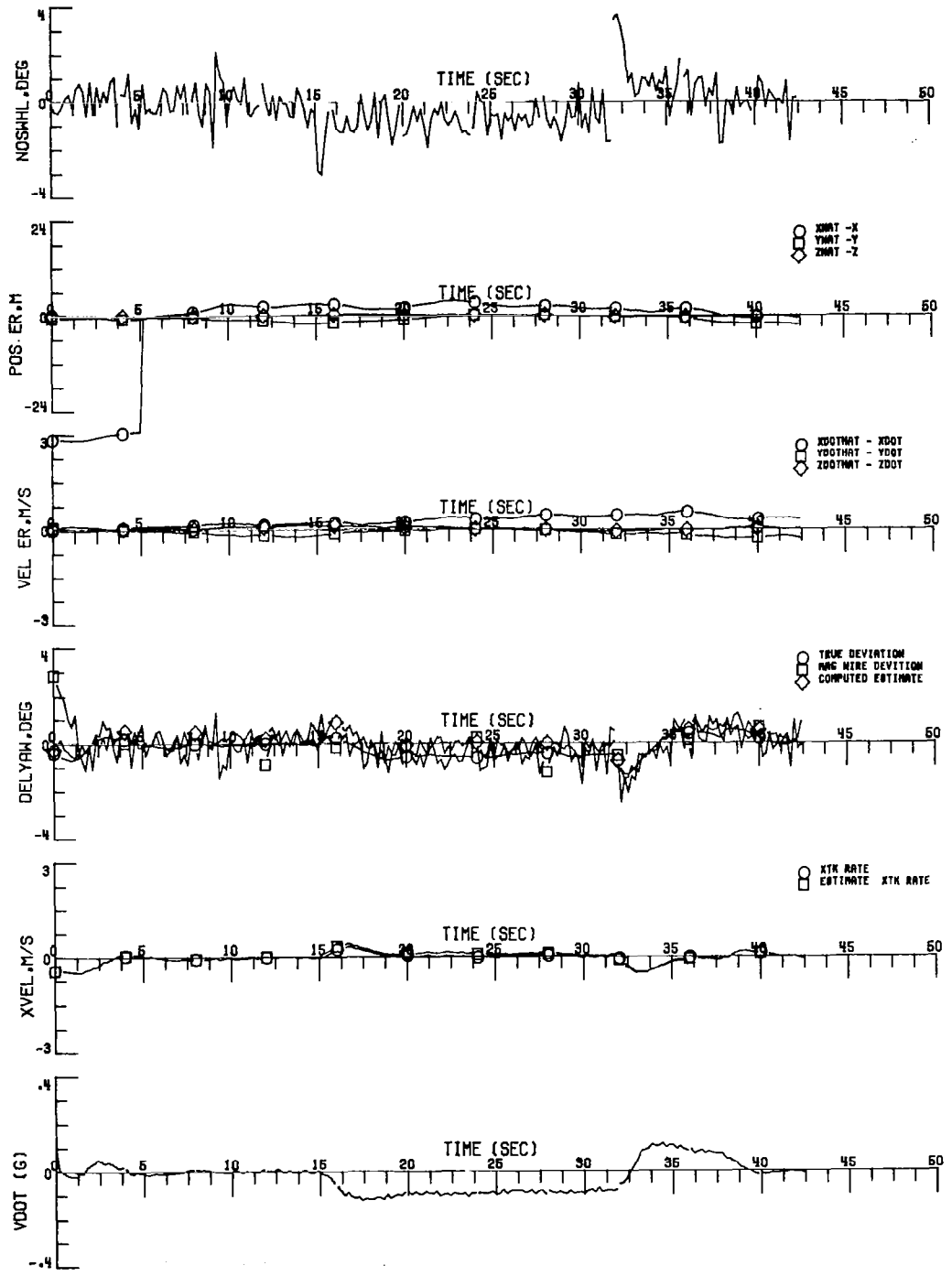

Figure 17. (Concluded)

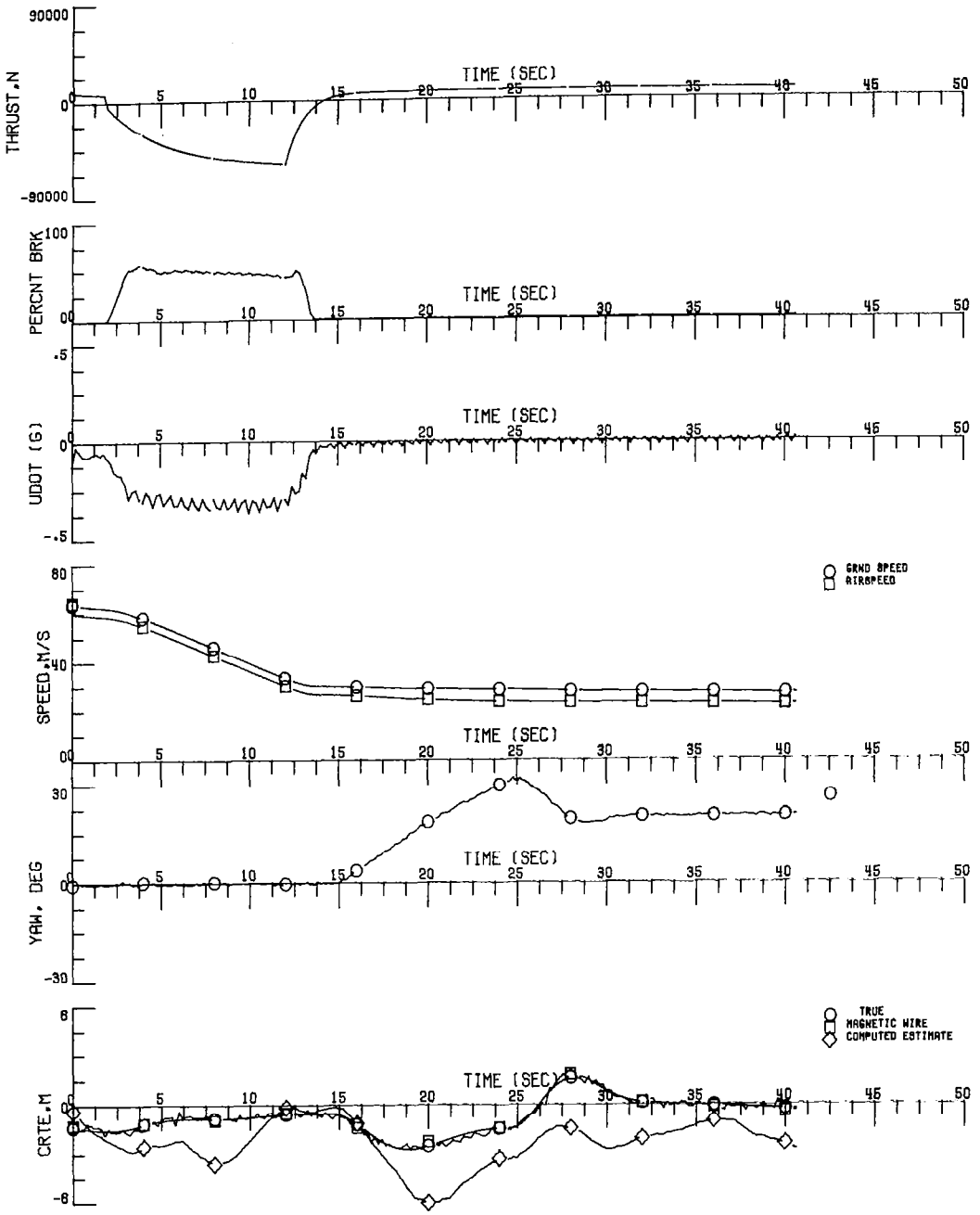

Figure 18. Rollout and Turnoff on Dry Runway - Noise and Bias Acting

Turn Speed = 65 knots
Taxi Speed = 60 knots
Winds = 10 knots at 45° heading
Turn Radius = 548.6 m
Landing Wt. = 40823.3 kg
Kalman Filter Used

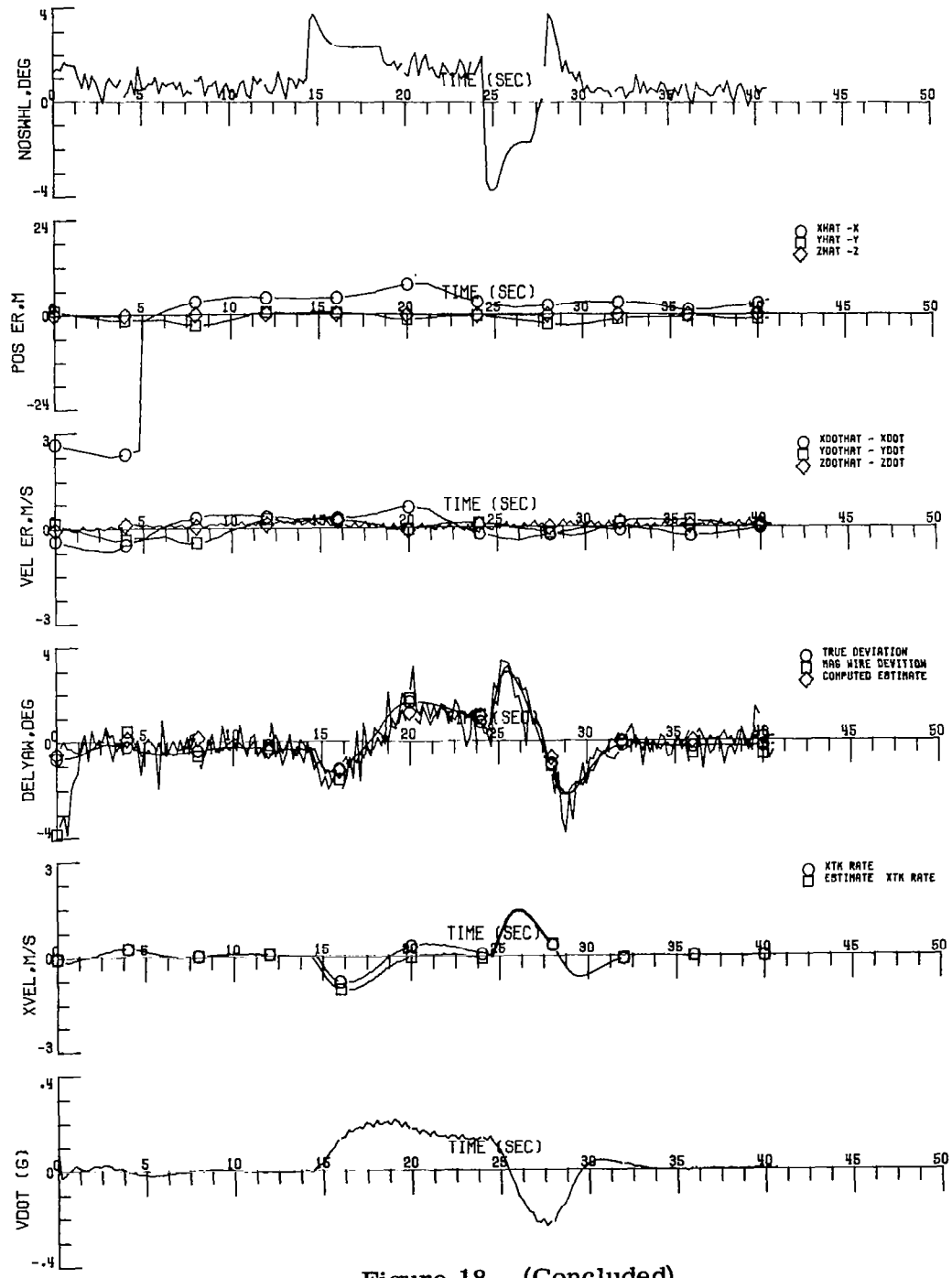

Figure 18. (Concluded)

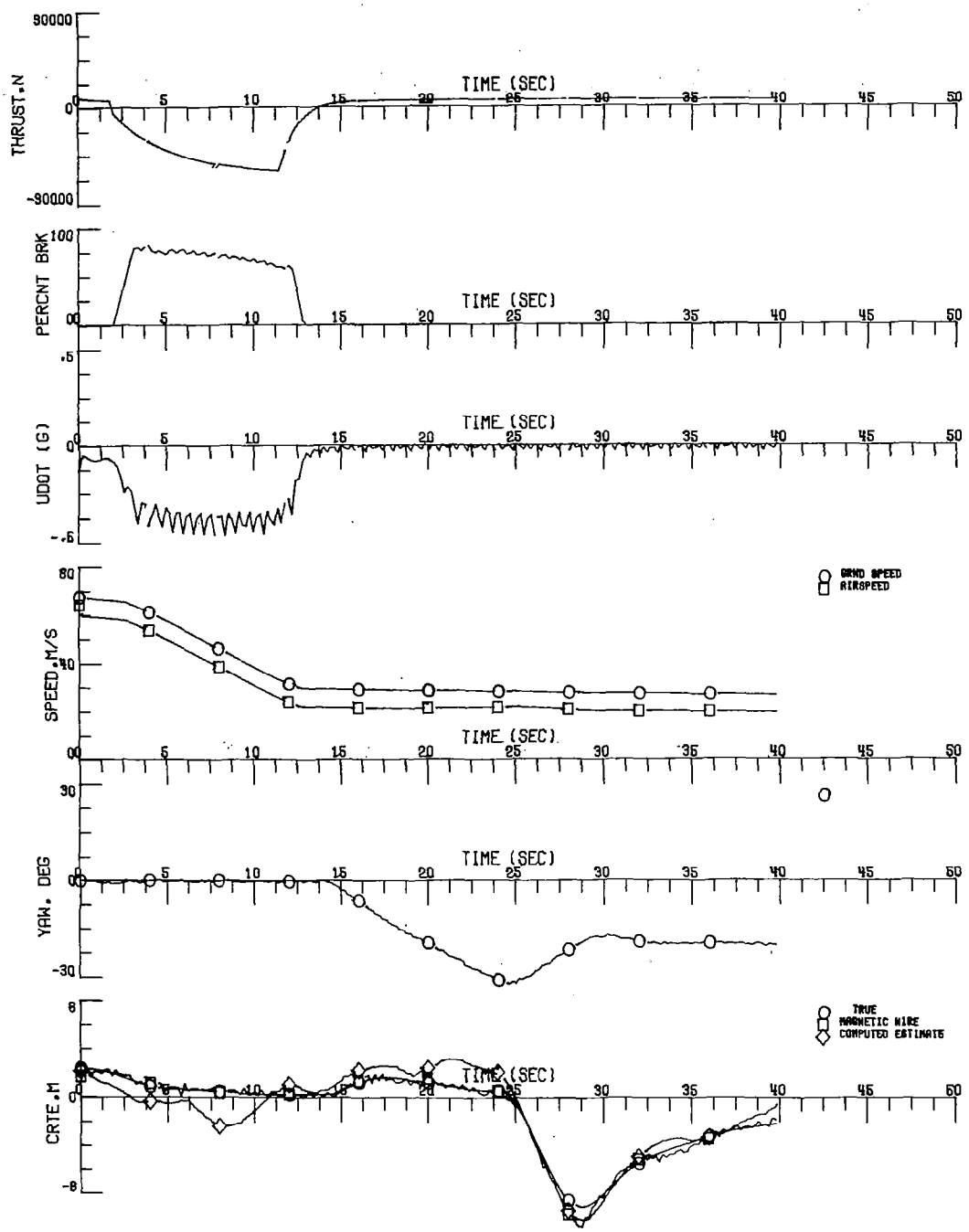

Figure 19. Rollout and Turnoff on Dry Runway – Noise and Bias Acting

Turn Speed = 65 knots
Taxi Speed = 60 knots
Winds = 15 knots at 0^{o} heading
Turn Radius = 548.6 m
Landing Wt. = 40823.3 kg
Kalman Filter Used

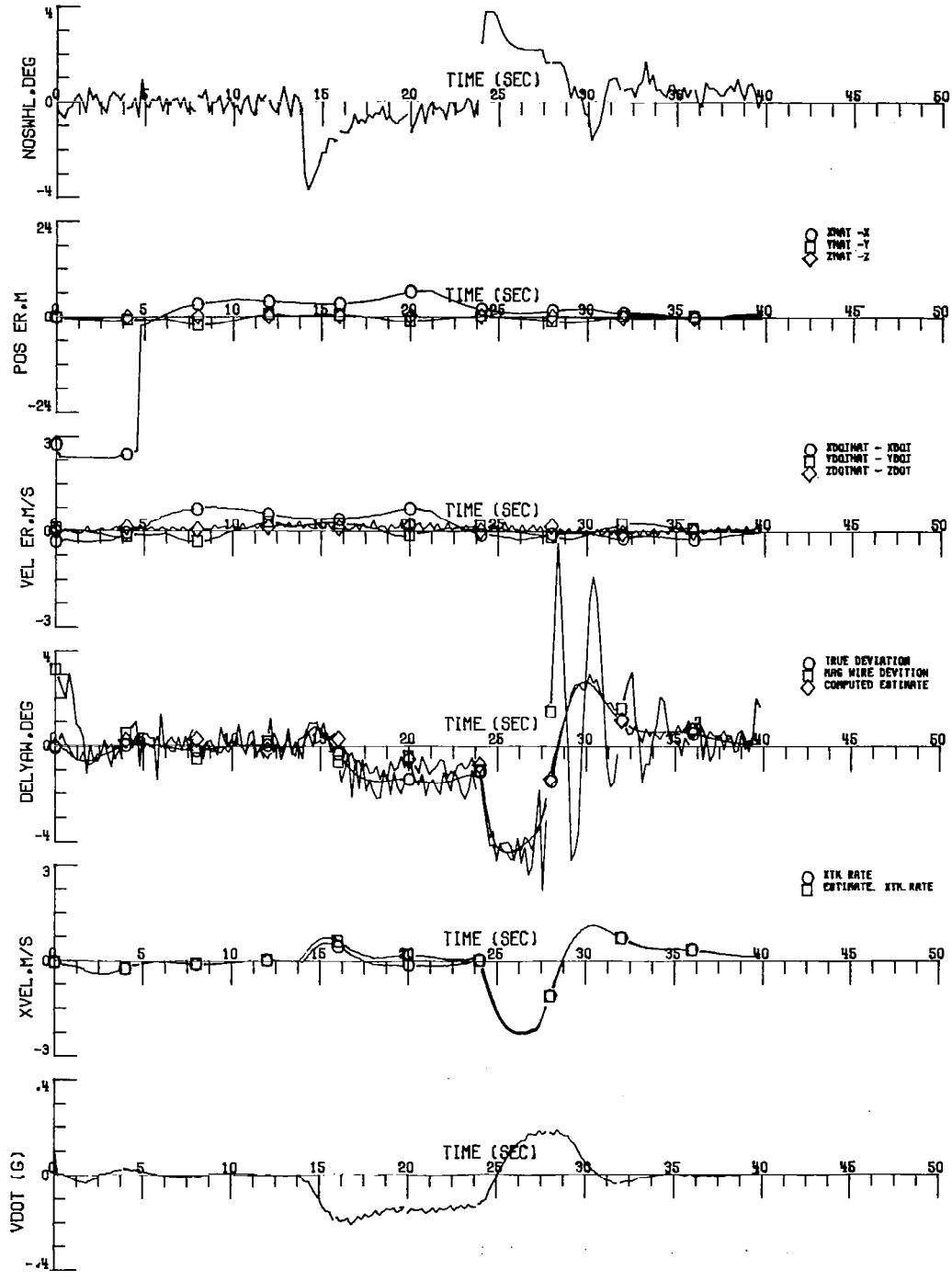

Figure 19. (Concluded)

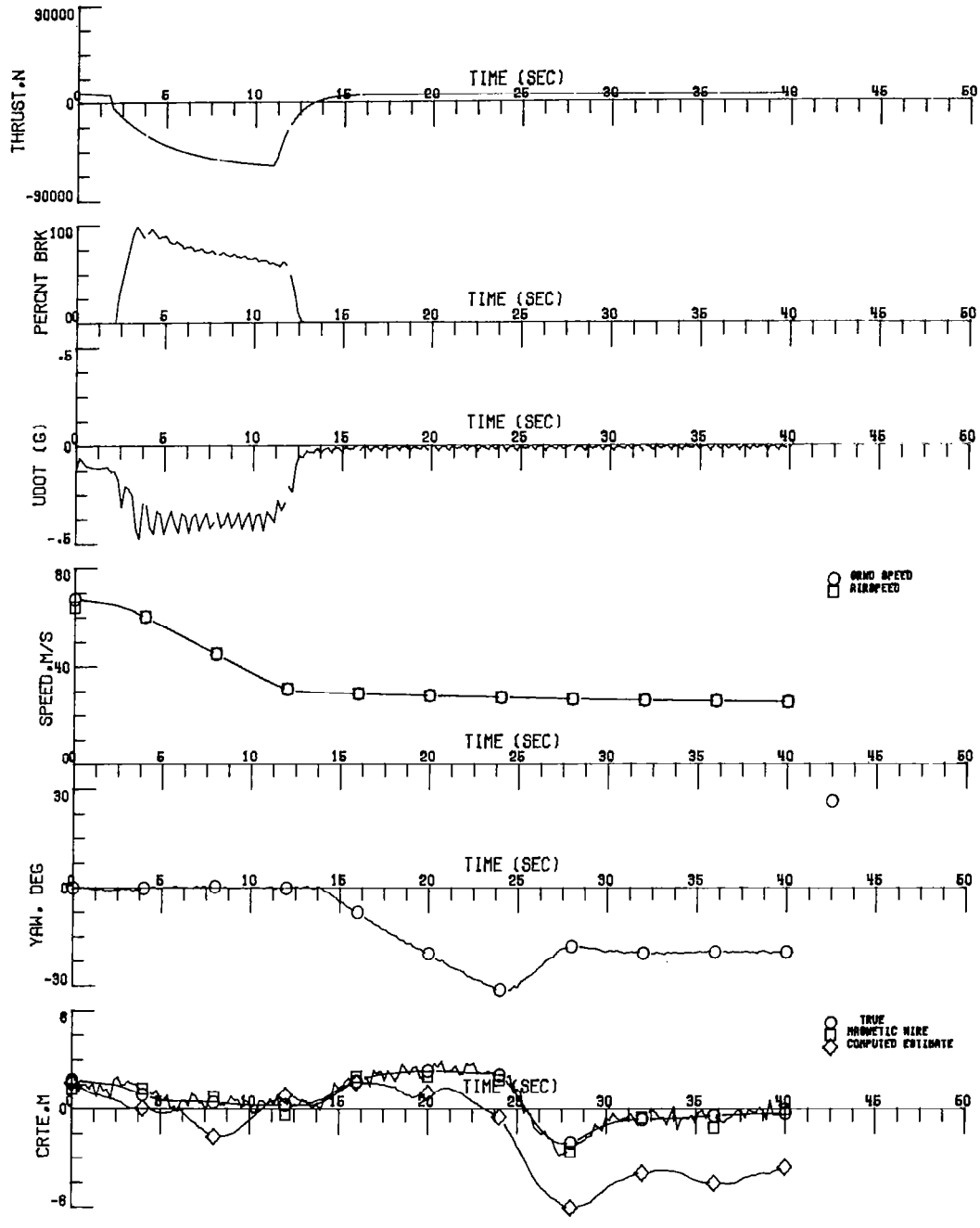

Figure 20. Rollout and Turnoff on Dry Runway - Excessive Noise and Bias Acting

Turn Speed = 65 knots
Taxi Speed = 60 knots
No Winds
Turn Radius = 548.6 m
Landing Wt. = 40823.3 kg
Complementary Filter Used

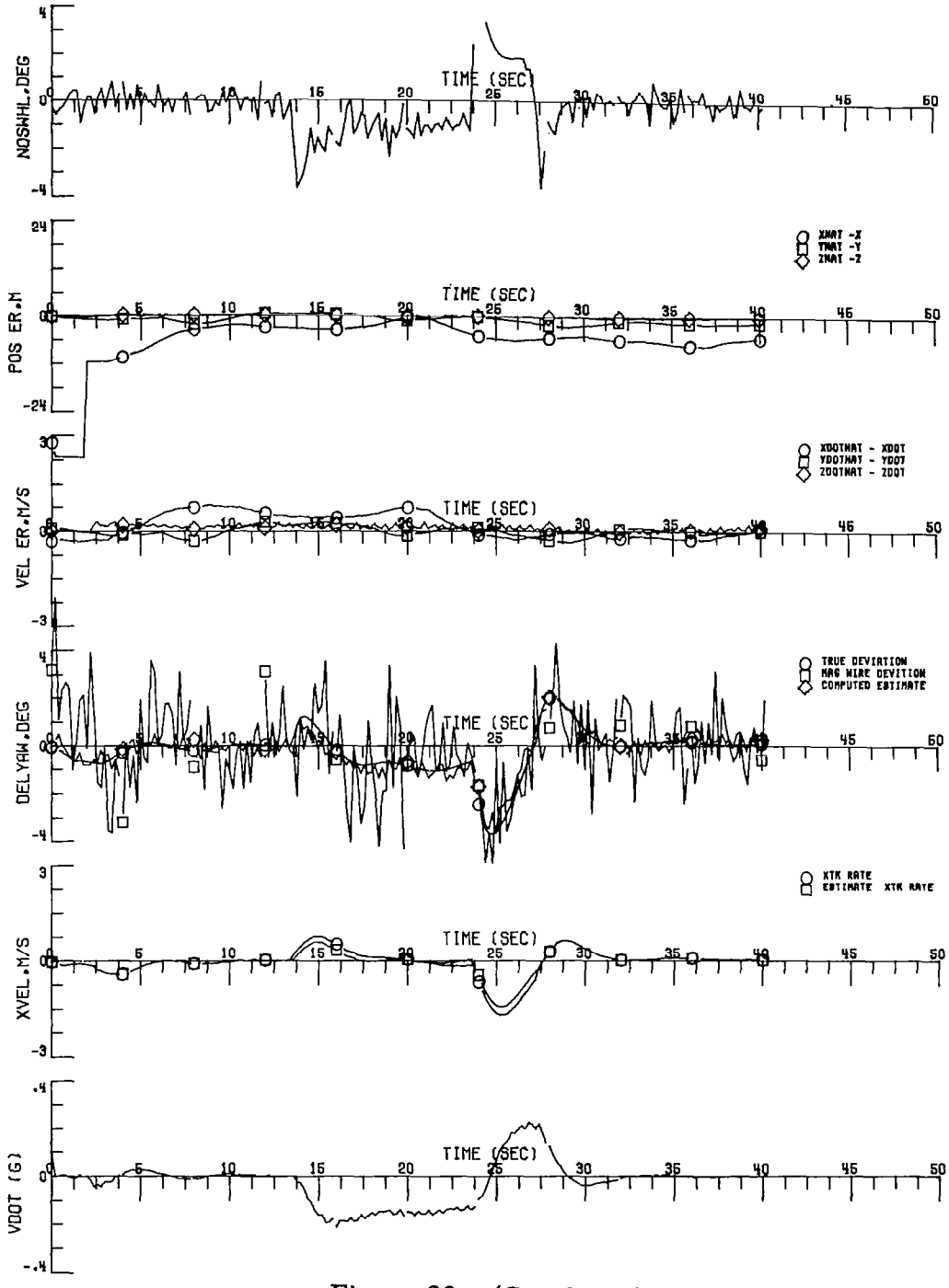

Figure 20. (Concluded)

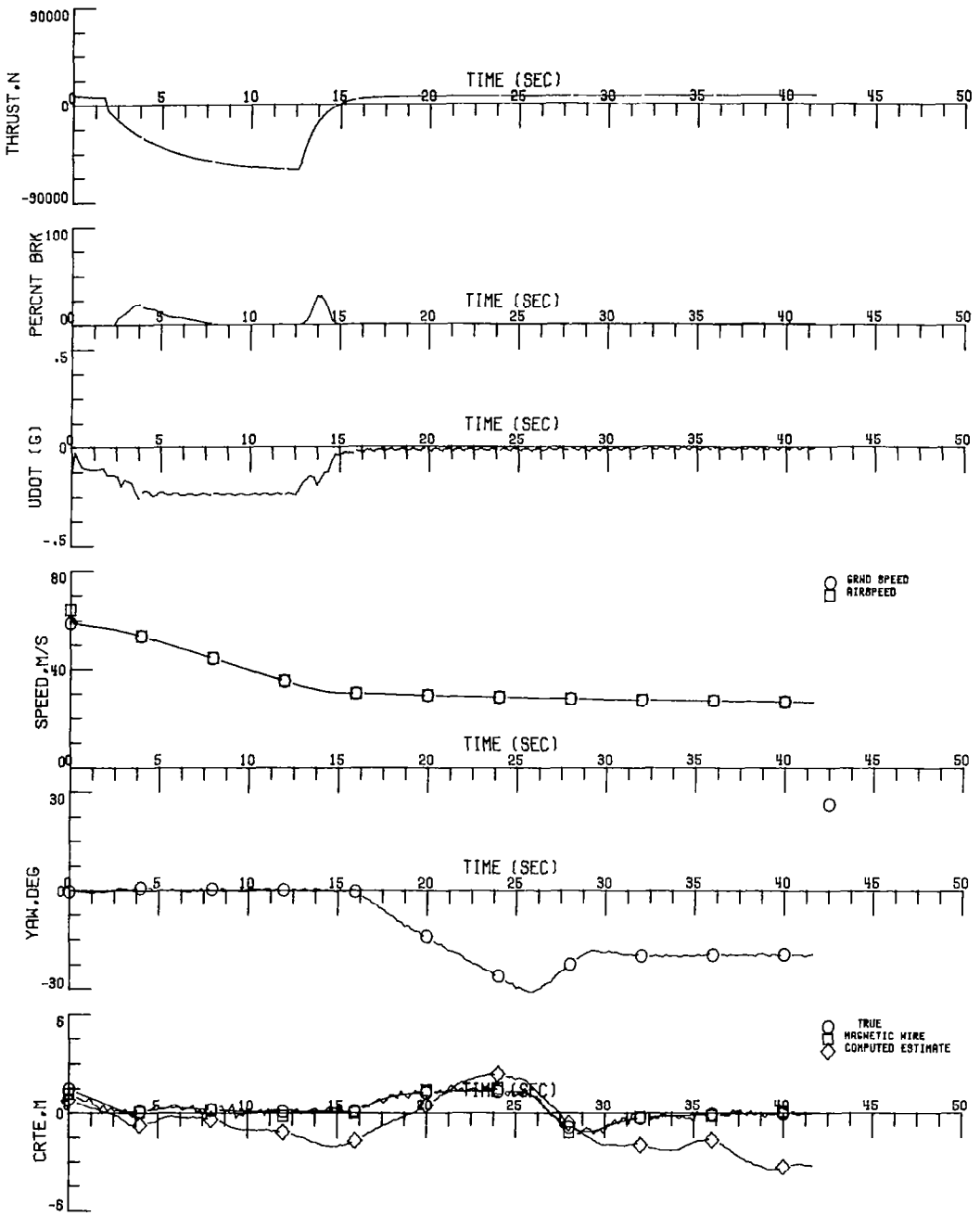

Figure 21. Rollout and Turnoff on Dry Runway - Noise and Bias Acting

Turn Speed = 65 knots
Taxi Speed = 60 knots
No Winds
Turn Radius = 548.6 m
Landing Wt. = 31751.5 kg
Complementary Filter Used

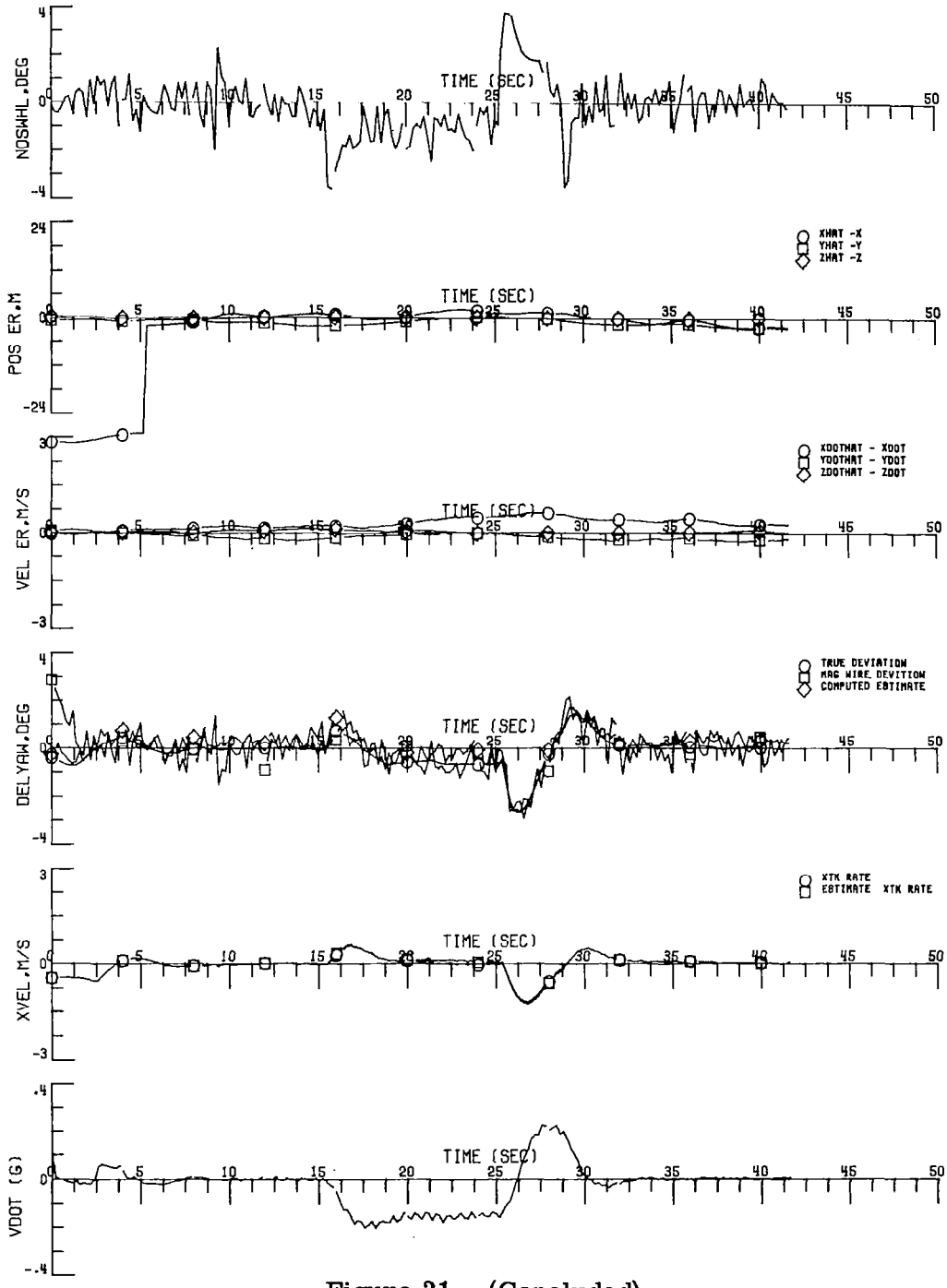

Figure 21. (Concluded)

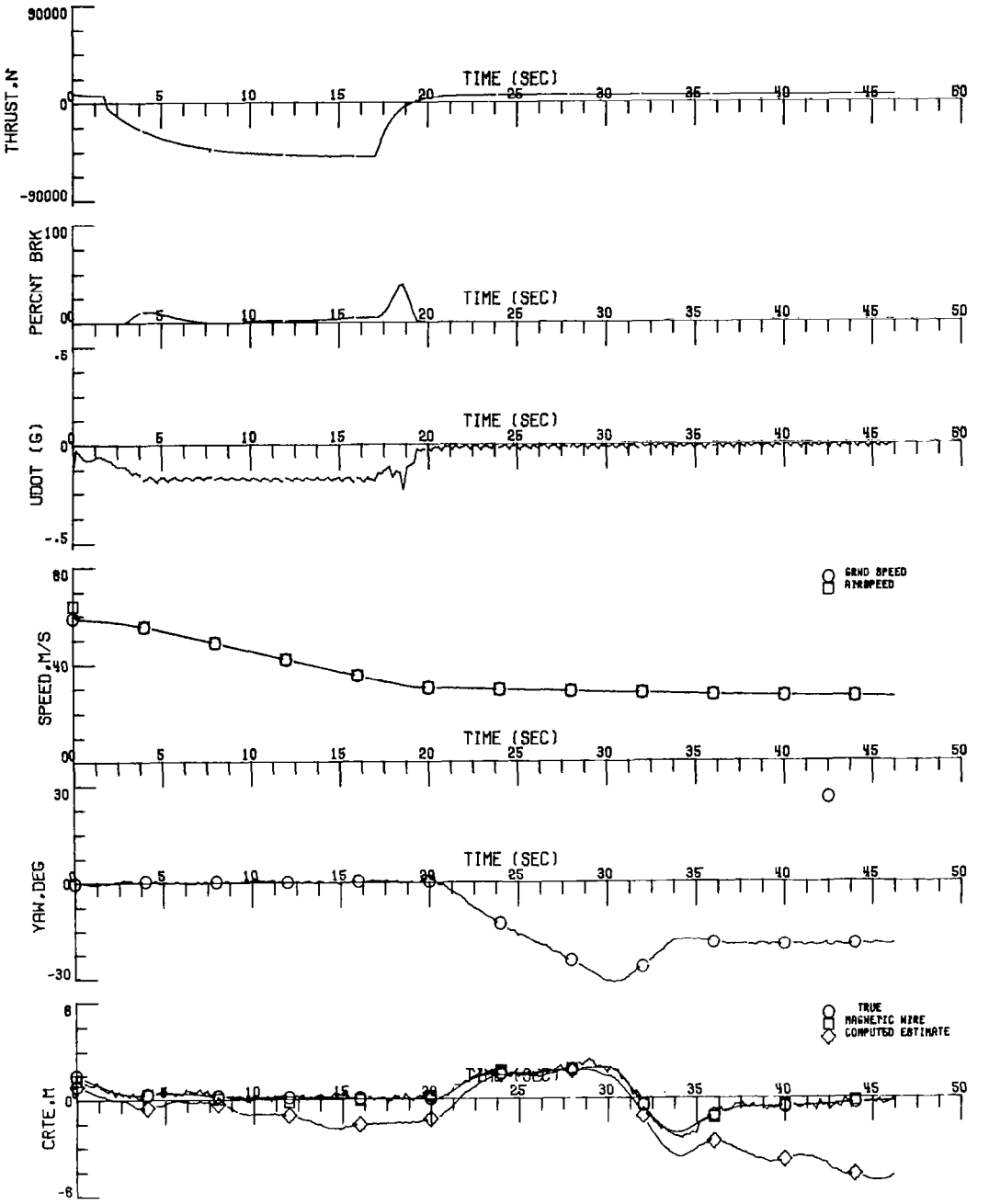

Figure 22. Rollout and Turnoff on Dry Runway - Noise and Bias Acting

Turn Speed = 65 knots
Taxi Speed = 60 knots
Rollout Distance to First Turn = 4500 feet
No Winds
Turn Radius = 548.64 m
Landing Wt. = 40823.3 kg
Complementary Filter Used

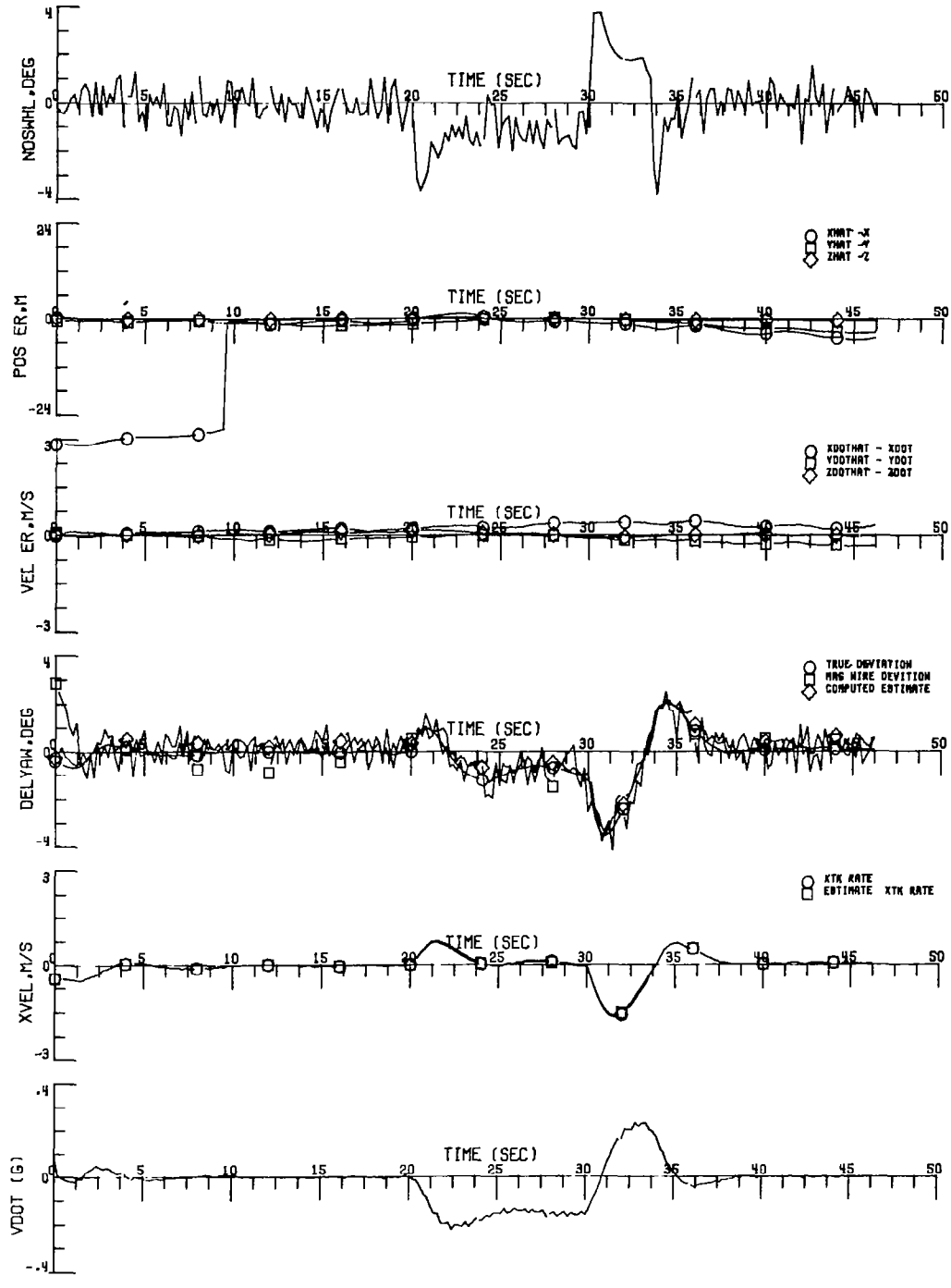

Figure 22. (Concluded)

APPENDIX A

RNAV EQUATIONS FOR PARABOLIC TURNS IN ROLLOUT AND TURNOFF

RNAV EQUATIONS FOR THE GENERAL RUNWAY CURVE

Let the runway coordinate system have its origin at the apron of the landing strip, with the x axis pointing north, the y axis due west, and z axis down. Yaw is measured clockwise from the north pointing x axis.

Let the prescribed curve, describing the required turnoff path, be given in the most general form

$$y_D = f(x_D) = \sum_{i=0}^{N} a_i x_D^i \tag{A1}$$

The required yaw for any point on the curve is given by

$$\tan \psi_D = \frac{dy_D}{dx_D} = \sum_{i=0}^{N} i\, a_i\, x_D^{i-1} \tag{A2}$$

To find the lateral deviation from the prescribed curve at some x, y point, not on the curve, we have

$$\delta = (y - y_D) \cos \psi_D - (x - x_D) \sin \psi_D \tag{A3}$$

It is necessary to determine x_D, y_D, and ψ_D, given x, y and the coefficients, a_i, defining the curve.

We have

$$\frac{x - x_D}{y - y_D} = -\frac{1}{dx_D/dy_D} = -\sum_{i=0}^{N} i\, a^i\, x_D^{i-1} \tag{A4}$$

Substituting Eq.(A1) for y_D into Eq.(A4) we have for the polynomial in x_D that must be solved,

$$x - x_D = -\left(y - \sum_0^N a_i x_D^i\right)\left(\sum_0^N i\, a_i x_D^{i-1}\right) \tag{A5}$$

It is plain that for a given curve of order N, the polynomial to be solved for in x_D is of order $2N - 1$. For $N > 2$ this will require some Newton iteration for real time processing of the RNAV equations. Such a computing burden is to be avoided, if possible.

For $N = 2$, the most general conic section requires a cubic. For the special case of the circle, only a quadratic equation need be solved; which accounts for its use in inflight RNAV. However, if we desire to avoid excessive abrupt lateral accelerations we must ease into the turn and other conic sections should be examined.

For the centered parabola we obtain a cubic which we may guarantee has only one real root for reasonable deviations from the prescribed curve.

We define a centered parabola as

$$u_D = \frac{1}{2R_o} v_D^2 \operatorname{sgn}(\psi_f - \psi_o) \tag{A6}$$

where R_o is the minimum radius of curvature at the point (o , o) , and $\operatorname{sgn}(\psi_f - \psi_o)$ is the sign of the difference between the required yaw at the end of the turn and required yaw and the beginning of the turns.

The angle between the tangent to the centered parabola and the v axis is given by

$$\frac{d u_D}{d v_D} = \tan \beta_D = \frac{\operatorname{sgn}(\psi_f - \psi_o)\, v_D}{R_o} \tag{A7}$$

To obtain the lateral deviation from the prescribed u_D, v_D curve at a point (u, v), not on the curve, we have

$$v_D^3 + 2R_o \left(R_o - \text{sgn} (\psi_f - \psi_o) u \right) v_D - 2R_o^2 v = 0 \tag{A8}$$

The solution of Eq. (A8) will have one real root provided

$$\text{sgn} (\psi_f - \psi_o) u < R_o - (27/4 R_o v^2)^{1/3} \tag{A9}$$

For reasonable distances from the prescribed curve, only one real solution exists and it is given by

$$v_D = A \Big/ |A|^{2/3} + B \Big/ |B|^{2/3} \tag{A10}$$

where

$$A = - Q/2 + \left(\frac{4P^3 + 27Q^2}{108} \right)^{1/2}$$

$$B = - Q/2 - \left(\frac{4P^3 + 27Q^2}{108} \right)^{1/2} \tag{A10a}$$

and

$$Q = - 2 R_o^2 v$$

$$P = 2 R_o \left(R_o - \text{sgn} (\psi_f - \psi_o) u \right) \tag{A10b}$$

The corresponding value of u_D is given by Eq. (A6).

$$u_D = \text{sgn} (\psi_f - \psi_o) v_D^2 \Big/ 2 R_o \tag{A6}$$

To express u , v in terms of the runway coordinates, we have

$$\begin{Bmatrix} v \\ u \end{Bmatrix} = \begin{pmatrix} \cos\alpha & \sin\alpha \\ -\sin\alpha & \cos\alpha \end{pmatrix} \begin{Bmatrix} x - x_o \\ y - y_o \end{Bmatrix} + \text{sgn}\,(\psi_f - \psi_o)\, R_o \begin{Bmatrix} \tan\left(\frac{\psi_o - \psi_f}{2}\right) \\ \frac{1}{2}\tan^2\left(\frac{\psi_o - \psi_f}{2}\right) \end{Bmatrix} \tag{A11}$$

where

x_o , y_o are the initial runway coordinates at the start of the turn, and α is the average yaw angle,

$$\alpha = \frac{\psi_f + \psi_o}{2} \tag{A11a}$$

To obtain the cross track error we have from Eq. (3)

$$\text{CTRE} = \delta = (u - u_D)\cos\beta_D - (v - v_D)\sin\beta_D \tag{A12}$$

where

$$\cos\beta_D = \frac{R_o}{(R_o^2 + v_D^2)^{\frac{1}{2}}}$$

$$\sin\beta_D = \frac{\text{sgn}\,(\psi_f - \psi_o)\, v_D}{(R_o^2 + v_D^2)^{\frac{1}{2}}} \tag{A12a}$$

u, v are obtained from the runway coordinates (x, y) by Eq. (11) and u_D , v_D , $\cos\psi_D$, and $\sin\psi_D$ are the solutions of the cubic given by Eqs. (A10), (A6), and (A12a).

The track angle error is obtained from

$$\text{TAGE} = \psi - \psi_D \tag{A13}$$

where ψ is the true yaw

and

$$\psi_D = \beta_D + \alpha \tag{A13a}$$

A useful formula for the track angle error is given by

$$TAGE = \tan^{-1}\left(\frac{\sin\psi \cos\psi_D - \cos\psi \sin\psi_D}{\cos\psi \cos\psi_D + \sin\psi \sin\psi_D} \right) \tag{A14}$$

The required yaw rate is given by

$$\dot{\psi}_D = v_G \, \mathrm{sgn}(\psi_f - \psi_o) \Big/ \left((R_o^2 + v_D^2)^{3/2} / R_o^2 \right) \tag{A15}$$

The expression in the denominator, $(R_o^2 + v_D^2)^{3/2} / R_o^2)$, is the radius of curvature of a point on the parabola (u_D , v_D). The sharpest turn is seen to lie in the center of the turn as desired.

The required cross track error rate is given by

$$\begin{aligned} \dot{\delta} = {} & \cos\psi_D \, \dot{y} - v \cos\beta_D \, \dot{\psi}_D - \sin\psi_D \, \dot{x} - u \sin\beta_D \, \dot{\psi}_D \\ & + \dot{\psi}_D \, \frac{R_o}{2} \, \mathrm{sgn}(\psi_f - \psi_o) \sin\beta_D (1 + \sec^2\beta_D) \end{aligned} \tag{A16}$$

To obtain the distance to go to the end of the turn we have

$$DSTGO = \tfrac{1}{2} \, \mathrm{sgn}(\psi_f - \psi_o) \, R_o \left\{ \begin{array}{l} \tan\beta_f \sec\beta_f + \ln(\tan\beta_f + \sec\beta_f) \\ -\tan\beta_D \sec\beta_D - \ln(\tan\beta_D + \sec\beta_D) \end{array} \right\} \tag{A17}$$

where $\beta_f = \dfrac{\psi_f - \psi_o}{2}$

$$\text{and} \begin{cases} \tan \beta_D = \dfrac{\text{sgn}\,(\psi_f - \psi_o)\, v_D}{R_o} \\ \sec \beta_D = \dfrac{R_o}{(R_o^2 + v_D^2)^{\frac{1}{2}}} \end{cases} \tag{A17a}$$

It is convenient to relate the maximum radius of curvature, R_o, to the equivalent circular radius of curvature between the same two end points.

We have for the parabola

$$R_o = \left| \frac{\cos \alpha\,(x_f - x_o) + \sin \alpha\,(y_f - y_o)}{2 \tan\left(\dfrac{\psi_f - \psi_o}{2}\right)} \right| \tag{A18}$$

For the circle through the same end points

$$R_c = \left| \frac{(\cos \psi_f - \cos \psi_o)\,(x_f - x_o) - (\sin \psi_f - \sin \psi_o)\,(y_f - y_o)}{2(\cos \psi_f - \cos \psi_o)\,(\sin \psi_f - \sin \psi_o)} \right| \tag{A19}$$

Figure 23 illustrates the two curves through the same end points.

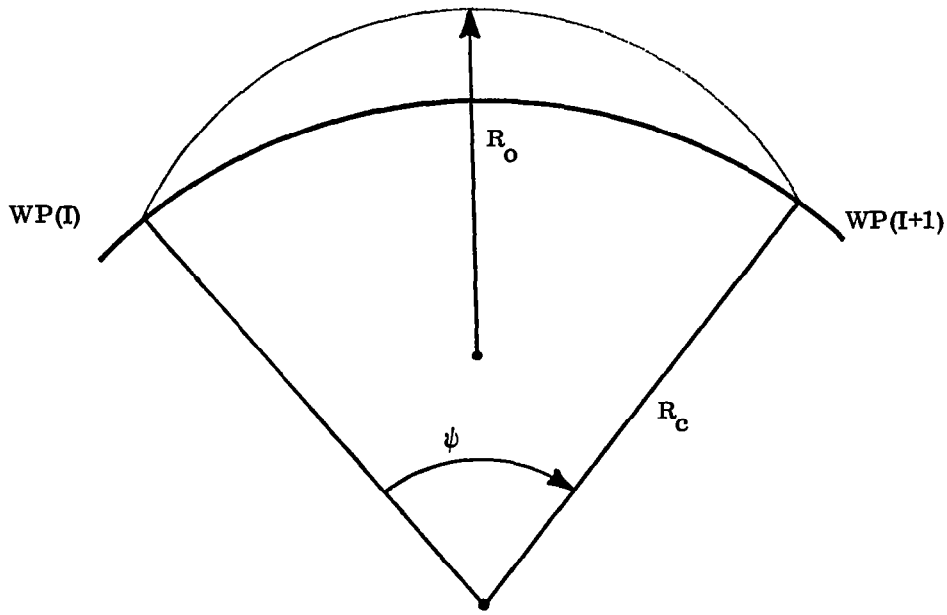

Figure 23. Circular vs Parabolic Turn

REFERENCES

1. Horne, Walter B.; McCarty, John L.; and Tanner, John A.; "Some Effects of Adverse Weather Conditions on Performance of Airplane Antiskid Braking Systems". NASA TN D-8202, 1976.

2. Pines, S.; Schmidt, S. F.; and Mann, F.; "Automated Landing, Rollout and Turnoff Using MLS and Magnetic Cable Sensors". NASA CR-2907, 1977.

3. Olsen, K.; Ventola, R.; and Pines, S.; "Tests of Magnetic Leader Cable and Sensors as a Rollout Navigational Aid". Analytical Mechanics Associates, Inc., Report No. 77-22, Nov. 1977.

4. Hueschen, R. M.; Creedon, J. F.; Bundick, W. T.; and Young, J. C.; "Guidance and Control System Research for Improved Terminal Area Operations," Presented at the 1980 Aircraft Safety and Operating Problems Conference at Hampton, Virginia, November 5-7, 1980.

1. Report No.	2. Government Accession No.	3. Recipient's Catalog No.
NASA CR-3451		

4. Title and Subtitle	5. Report Date
TERMINAL AREA AUTOMATIC NAVIGATION, GUIDANCE, AND CONTROL RESEARCH USING THE MICROWAVE LANDING SYSTEM (MLS) PART 1 - AUTOMATIC ROLLOUT, TURNOFF, AND TAXI	August 1981
	6. Performing Organization Code

7. Author(s)	8. Performing Organization Report No.
Samuel Pines	AMA 80-1
	10. Work Unit No.

9. Performing Organization Name and Address	11. Contract or Grant No.
Analytical Mechanics Associates, Inc. 17 Research Road Hampton, Virginia 23666	NAS1-15116
	13. Type of Report and Period Covered
12. Sponsoring Agency Name and Address	Contractor Report
National Aeronautics and Space Administration Washington, DC 20546	14. Sponsoring Agency Code

15. Supplementary Notes

Langley Technical Monitor: Richard M. Hueschen
Final Report

16. Abstract

This report contains the results of a study developed for the Langley TCV B-737 program to apply existing navigation aids plus magnetic leader cable signals and develop braking and reverse thrust guidance laws to provide for rapid automated rollout, turnoff, and taxi to reduce runway occupation time for a wide variety of landing conditions for conventional commercial-type aircraft.

Closed loop guidance laws for braking and reverse thrust are derived for rollout, turnoff, and taxi, as functions of the landing speed, the desired taxi speed and the distance to go. Brake limitations for wet runway conditions and reverse thrust limitations are taken into account to provide decision rules to avoid tire skid and to choose an alternate turnoff point, farther down the runway, to accommodate extreme landing conditions.

17. Key Words (Suggested by Author(s))	18. Distribution Statement
Rollout Turnoff Braking Reverse thrust Steering guidance	Unclassified - Unlimited Subject Category 08

19. Security Classif. (of this report)	20. Security Classif. (of this page)	21. No. of Pages	22. Price
Unclassified	Unclassified	79	A05

For sale by the National Technical Information Service, Springfield, Virginia 22161

NASA-Langley, 1981